REPORT NO. NADC-83062-40

A133168

THEORETICAL PREDICTIONS FOR VLF RADIO PROPAGATION

Dr. M. P. Paul
Communication Navigation Technology Directorate (Code 4044)
NAVAL AIR DEVELOPMENT CENTER
Warminster, PA 18974

8 AUGUST 1983

PHASE REPORT
Task No. X10830003
Work Unit No. CY930

APPROVED FOR PUBLIC RELEASE; DISTRIBUTION UNLIMITED.

Prepared for
NAVAL ELECTRONICS SYSTEMS COMMAND (PME-410-112)
Department of the Navy
Washington, DC 20360

NOTICES

REPORT NUMBERING SYSTEM – The numbering of technical project reports issued by the Naval Air Development Center is arranged for specific identification purposes. Each number consists of the Center acronym, the calendar year in which the number was assigned, the sequence number of the report within the specific calendar year, and the official 2-digit correspondence code of the Command Office or the Functional Directorate responsible for the report. For example: Report No. NADC-78015-20 indicates the fifteenth Center report for the year 1978, and prepared by the Systems Directorate. The numerical codes are as follows:

CODE	OFFICE OR DIRECTORATE
00	Commander, Naval Air Development Center
01	Technical Director, Naval Air Development Center
02	Comptroller
10	Directorate Command Projects
20	Systems Directorate
30	Sensors & Avionics Technology Directorate
40	Communication & Navigation Technology Directorate
50	Software Computer Directorate
60	Aircraft & Crew Systems Technology Directorate
70	Planning Assessment Resources
80	Engineering Support Group

PRODUCT ENDORSEMENT – The discussion or instructions concerning commercial products herein do not constitute an endorsement by the Government nor do they convey or imply the license or right to use such products.

APPROVED BY: William F. Lyons Jr. DATE: 15 August 1983

Unclassified

SECURITY CLASSIFICATION OF THIS PAGE (When Data Entered)

REPORT DOCUMENTATION PAGE

READ INSTRUCTIONS BEFORE COMPLETING FORM

1. REPORT NUMBER NADC - 83062-40	2. GOVT ACCESSION NO. A133168
3. RECIPIENT'S CATALOG NUMBER	
4. TITLE (and Subtitle) THEORETICAL PREDICTIONS FOR VLF RADIO PROPAGATION	5. TYPE OF REPORT & PERIOD COVERED Phase Report
	6. PERFORMING ORG. REPORT NUMBER
7. AUTHOR(s) Dr. M. P. Paul	8. CONTRACT OR GRANT NUMBER(s)
9. PERFORMING ORGANIZATION NAME AND ADDRESS Communications Navigation Technology Directorate Naval Air Development Center (Code 4044) Warminster, PA 18974	10. PROGRAM ELEMENT, PROJECT, TASK AREA & WORK UNIT NUMBERS Task No X10830003
11. CONTROLLING OFFICE NAME AND ADDRESS NAVAL ELECTRONICS SYSTEMS COMMAND (ELEX- Department of the Navy, Washington, D.C. 20360	12. REPORT DATE 22 August, 1983
	13. NUMBER OF PAGES 74
14. MONITORING AGENCY NAME & ADDRESS (if different from Controlling Office)	15. SECURITY CLASS. (of this report) Unclassified
	15a. DECLASSIFICATION/DOWNGRADING SCHEDULE

16. DISTRIBUTION STATEMENT (of this Report)

Approved for public release; distribution unlimited.

17. DISTRIBUTION STATEMENT (of the abstract entered in Block 20, if different from Report)

18. SUPPLEMENTARY NOTES

19. KEY WORDS (Continue on reverse side if necessary and identify by block number)

EM Propagation
Very Low Frequency
Earth Ionosphere Waveguide Mode

20. ABSTRACT (Continue on reverse side if necessary and identify by block number)

The very low frequency (VLF, 3 to 30 kHz) part of the radio frequency spectrum is characterized by low attenuation rate, high phase and frequency stability, and high signal to noise ratio. Consequently, VLF radio propagation is used for many practical applications, e.g., frequency standardization, clock synchronization, and reliable long-distance radio communications. Because of the distinct advantages of VLF radio —

(over)

DD FORM 1 JAN 73 1473 EDITION OF 1 NOV 65 IS OBSOLETE
S/N 0102-LF-014-6601

Unclassified

SECURITY CLASSIFICATION OF THIS PAGE (When Data Entered)

propagation, the U.S. Navy will be conducting a balloon-to-balloon-borne cross link communication experiment to study the characteristics of VLF high altitude radio propagation.

In this Technical Report, an attempt has been made to make theoretical computations of the vertical components of the individual and multimode field strengths as a function of distance based on mode theory. The variations of various ionospheric parameters, e.g., attenuation rates, the heights of the ionospheric reflection point, the height gain factors for an appropriate combination of the transmitting and receiving antenna elevations, along with the presence of the earth's geomagnetic field, especially for the East-West propagation, have been duly considered. The results obtained have been presented in tabular and graphical forms and are consistent with the values obtained by earlier workers. These field strength values will be compared against the experimental values when the above-mentioned ambitious experiment is carried out in the Pacific in the late Summer of 1983.

TABLE OF CONTENTS

ACKNOWLEDGEMENT

The research work reported in this Technical Report was carried out during the Summers of 1982 and 1983 while the author was working as an ASEE-Navy Summer Faculty Research Fellow under the sponsorship of the American Society for Engineering Education, Washington, D.C. The author gratefully acknowledges the hospitality that he has enjoyed at the Naval Air Development Center, Warminster, Pennsylvania, where this work was carried out. He also takes this opportunity to express his sincere thanks to many of his host colleagues, especially, Messers J. Pye, E. Wykes, L. Newman, J. Paynter and Dr. G. Palatucci, for technical help and scientific discussions. Special thanks are also due to the author's university, Alcorn State University, Lorman, Mississippi, for releasing him during the two summer sessions while this investigation was being carried out.

ABSTRACT

The very low frequency (VLF, 3 to 30 KHz) part of the radio frequency spectrum is characterized by low attenuation rate, high phase and frequency stability, and high signal to noise ratio. Consequently, VLF radio propagation is used for many practical applications, e.g., frequency standardization, clock synchronization, and reliable long-distance radio communications. Because of the distinct advantages of VLF radio propagation, the U.S. Navy will be conducting a balloon-to-balloon-borne cross link communication experiment to study the characteristics of the VLF high altitude radio propagation.

In this technical report, an attempt has been made to make theoretical computations of the vertical components of the individual and multimode field strengths as a function of distance based on mode theory. The variations of various ionospheric parameters, e.g., attenuation rates, the height of the ionospheric reflection point, the height gain factors for an appropriate combination of the transmitting and receiving antenna elevations, along with the presence of the earth's geomagnetic field, especially for the East-West propagation, have been duly considered. The results obtained have been presented in tabular and graphical form and are consistent with the values obtained by earlier workers. These field strength values will be compared against the experimental values when the above-mentioned ambitious experiment is carried out in the Pacific in the late Summer of 1983.

LIST OF ILLUSTRATIONS

LIST OF ILLUSTRATIONS (CONTINUED)

LIST OF ILLUSTRATIONS (CONTINUED)

LIST OF ILLUSTRATIONS (CONTINUED)

LIST OF TABLES

LIST OF TABLES (CONTINUED)

INTRODUCTION

Analogous to microwave propagation along a waveguide, very low frequency (VLF, 3 to 30 KHz) radio propagation over long distance is treated as if the propagation takes place in a terrestrial spherical waveguide with boundaries formed by the conducting earth's surface and the lower edge of the reflecting ionosphere. For the frequency range under consideration, (15 to 30 KHz, i.e., the upper band of the VLF spectrum) the analysis of the wave propagation is simplified because of the limited number of significant modes that need to be considered. The level of excitation of the individual modes depends upon the corresponding excitation factors and the variation of field strengths across the waveguide cross-section as given by the so-called height gain functions. For lower order modes (especially say, the first order mode) the energy of the wave is mostly concentrated at the base of the ionosphere. For such a mode, the excitation factor is small, which implies inefficiency for launching such a wave from a ground-based point as the excitation factor for such a wave will not depend much on ground conductivity. However, as it turns out, the height gain factors for such waves increase as the height of the transmitting antenna increases. The waves become earth-detached and are called earth-detached modes (nomenclature due to James R. Wait) or whispering gallery modes (nomenclature due to K. G. Budden). Such waves, naturally characterized with very low attenuation rates, criss-cross the ionosphere without any intermediate earth-based bouncing point and propagate over long distances without losing much of their energy.

The U.S. Navy is planning a balloon-to-balloon communication link experiment employing this mode of propagation. The plans for this experiment have been given elsewhere (3). In this technical report, only the theoretically computed values of the vertical field components of the field strength radiated out by a vertically polarized antenna at different distances for different configurations of the transmitting and receiving antenna heights will be presented.

THEORY

The theory of very low frequency radio propagation has been thoroughly discussed in many well known texts and research reports (2,4,5,6 and 7). Several approximation theories can be utilized in order to limit the mathematical sophistication within bounds. In this consideration, the earth-ionosphere terrestrial waveguide is considered as a thin spherical shell. Spherical coordinate system (r,θ,ϕ) is used and the boundary conditions at the two interfaces are defined by their impedance conditions, i.e.,

$$Z_g = \frac{E_\theta}{H_\phi} \quad ; \quad Z_i = -\frac{E_\theta}{H_\phi}$$

where Z_g = impedance of the conducting ground

Z_i = impedance of the conducting ionosphere

E_θ = tangential electric field component

$H\phi$ = zonal magnetic field component

Furthermore, for special interest, discussion will be restricted to two discrete frequencies, 19.4 and 27 kHz, as these are the two frequencies which will be operational during the balloon-to-balloon-borne cross link communication experiment. Two levels of transmitter power will be used, one kilowatt and 440 watts. (For details, please refer to (3)). The ionosphere will be characterized with an exponential profile having a conductivity gradient $\ell = 2$ (or $\beta = 0.5$), where is the length over which ionospheric conductivity, which is a measure of the ratio ω_0^2/ν or N/ν, changes by a ratio of 2.71, where ω_0 is the plasma frequency and ν is the collisonal frequency and N is the electron density in the ionospheric layer.

According to the formulations of WKB (or second order) approximations, the integral form of the modal equation or the resonance condition for mode propagation of spherical waves can be written as (2,4,6)

$$R_g(C_n)\, R_i(C_n')\, \exp\left(-2ik \int_0^h (C_n + 2z/a)^{1/2}\, dz + i\pi/2\right)$$

$$= \exp(-2in\pi) \qquad (1)$$

where $R_g(C_n)$ and $R_i(C_n)$ are the Fresnel reflection coefficients of the earth's surface and the ionospheric surface for the complex angles of incidences;

$$C_n = (1 - S_n^2)^{1/2} \quad ; \quad C_n' = (1 - S_n'^2)^{1/2}$$

The other constants are defined as follows:

k = propagation constant = $2\pi/\lambda$

a = radius of the earth surface

$z_o = -aC_n^2/2$

As stated by Wait (4), under this approximation, valid for the frequency range of our interest (20 to 30 kHz), the modal characteristics are independent of the electrical properties of the earth's surface and the modes are characterized as earth-detached mode in analogy to their counterparts in accoustics originally investigated by Lord Rayleigh at the turn of the present century.

The total phase given by the integral form of the modal equation consists of a "to and fro" path between the ionospheric reflection point at $z=h$ and a second reflecting point at $z = z_o$ a height embraced by a surface, called caustic surface, below which the waves of lower order modes becomes evanescent. The phase shift at the caustic accounts for $\pi/2$. The excitation factors for these modes for the ground-based launching points are very small.

Assuming earth's surface as a perfect electricconductor and the ionospheric surface as a perfect magnetic conductor (i.e., $R_g = 1$ and $R_i = -1$), equation (1) reduces to

$$-2ik \int_{z_o}^{h} (C_n^2 + 2z/a)^{1/2} dz + i\pi/2 = -2ni\pi + i\pi \qquad (2)$$

and the solution is:

$$C_n = \left(\frac{3\pi}{ka}(n - 1/4)\right)^{2/3} - 2h/a$$

where C_n specifies the resonance condition for the modes.

The expression for the amplitude of the vertical component of the electric field strength at a certain distance can be written as (2,6)

$$E_z = \frac{300}{h}\left(\frac{P_R \times \lambda}{a \text{ Sin } D/a}\right)^{1/2} \sum_n \Lambda_n G_n(z)\, G_n(\hat{z}) \qquad (3)$$

$$\exp(-\alpha_n D) \quad \text{volt/meter}$$

and the phase of the nth mode component relative to the antenna current is given by (6)

$$\phi_{E_{z,n}} = \pi/4 - \omega D/v_{p,n} + \phi_{\Lambda_n} \qquad (4)$$

where E_z = Modesum field strength amplitude in volt/meter

h = ionospheric height in meters

λ = c/f = wavelength in meters

P_R = radiated power in kilowatts

D = distance in meters

Λ_n = nth mode excitation factor

$G_n(z)$ = height gain factor for the transmitting antenna at height z meters

$G_n(\hat{z})$ = height gain factor for the receiving antenna at height z meters

α_n = nth mode attenuation constant in dB/megameter

$E_{z,n}$ = phase of the nth mode in radians

$\phi_{\Lambda n}$ = phase of the nth mode excitation factor in radians

ω = angular frequency of the wave in radians

$v_{p,n}$ = phase velocity of the nth mode in meters/second.

As noted earlier, for the frequency range under consideration (15-30 kHz), very few modes are important for consideration. Consequently, for the present prupose only the first three modes (mode 1 through 3) will be considered.

SINGLE MODE FIELD STRENGTH

We can express the field strength amplitude in dBv/m from equation (3) for the nth mode as (where n is either 1 or 2 or 3):

$$E_{zn} = 20 \text{ Log } (300) - 20 \text{ Log } (h) + 10 \text{ Log } P_R + 10 \text{ Log } (3X10^8)$$

$$-10 \text{ Log } (f) - 10 \text{ Log } (a \sin D/a) - \frac{\alpha_n D}{10^6}$$

$$+ \text{HGF} \quad \text{dBv/m} \qquad (5)$$

$$= 20 \text{ Log } (10^6) + 20 \text{ Log } (300) - 20 \text{ Log } (h)$$

$$+10 \text{ Log } (P_R) + 10 \text{ Log } (3X10^8) - 10 \text{ Log } (f)$$

$$-10 \text{ Log } (a \sin D/a) - \frac{\alpha_n D}{10^6}$$

$$+ \text{HGF} \quad \text{dB}\mu\text{v/m} \qquad (6)$$

For daytime condition (h = 70 km) and for frequency f = 19.4 kHZ and P_R = 1 kilowatt, equation (6) reduces to:

$$E_{z,n} = 54.3 - 10 \text{ Log } (a \sin D/a) - \alpha D$$

$$+ \text{HGF} \quad \text{dB}\mu\text{v/m.kw} \qquad (7)$$

and for nighttime condition (h = 90 km)

$$E_{z,n} = 53.1 - 10 \text{ Log } (a \sin D/a) - \alpha D$$

$$+ \text{HGF} \quad \text{dB}\mu\text{v/m.kw} \qquad (8)$$

Similarly, for the second frequency, f = 27 kHZ and for the day and nighttime conditions, the corresponding expressions are:

$$E_{z,n} = 52.3 - 10 \text{ Log } (a \sin D/a) - \alpha D$$

$$+ \text{HGF} \quad \text{dB}\mu\text{v/m.kw} \qquad (9)$$

(f = 27 kHZ, h = 70 km)

and

$$E_{z,n} = 50.9 - 10 \, \mathrm{Log}(a \sin D/a) - \alpha D + HGF \qquad dB\mu v/m.kw \qquad (10)$$

(f=27 kHz, h=90 km)

In equations (7) through (10), a and D are expressed in megameters and α is in dB/megameter (Mm). HGF is the modified height gain function for the nth order mode and is given by (2)

$$HGF = 20 \, \mathrm{Log} \left(\Lambda_n G_n(z) G_n(\hat{z}) \right) \; dB \qquad (11)$$

Following reference (2) we can write

$$\Lambda_n = \frac{y_o}{2 \, t_n^{1/2} (y_o - t_n)^{1/2}} \exp\left(- \frac{4}{3} t_n^{3/2}\right) \qquad (12)$$

$$G_n(z) = \sqrt{\pi} \; t_n^{1/4} A_i(t_n - z) \exp\left(+ \frac{2}{3} t_n^{3/2}\right) \qquad (13)$$

and

$$G_n(\hat{z}) = \sqrt{\pi} \; t_n^{1/4} A_i(t_n - \hat{z}) \exp\left(+ \frac{2}{3} t_n^{3/2}\right) \qquad (14)$$

where

$$y_o = (ka/2)^{2/3} (2h/a)$$

$$z = (ka/2)^{2/3} (h_T/a)$$

$$\hat{z} = (ka/2)^{2/3} (h_R/a)$$

$$t_n = (ka/2)^{2/3} (- C_n^2)$$

$$C_n^2 = \left(\frac{3\pi}{Ka} (n - 1/4)\right)^{2/3} - 2h/a$$

h_T = height of the transmitting antenna above the ground surface

h_R = height of the receiving antenna above the ground surface

$A_i(t_n - z)$ and $A_i(t_n - \hat{z})$ are the Airy functions of arguments $(tn - z)$ and $(t_n - \hat{z})$ as defined in reference (8).

The arguments (t_{n-z}) or ($t_{n-\hat{z}}$), since they are symmetrical, of the Airy functions can be simplified as follows:

$$t_{n-z} = \frac{(ka)^{2/3}}{2} \left[\frac{2h}{a} - \left[\frac{3\Pi}{ka}(n-1/4)\right]^{2/3} - \frac{2h_T}{a}\right]$$

$$= \frac{(2)}{a}\frac{(ka)^{2/3}}{2}(h-h_T) - \left(\frac{3\Pi}{2}\right)^{2/3}(n-1/4)^{2/3}$$

or

$$(t_{n-z}) = 5.15 \text{ X } 10^{-3}\ (h-h_T)f^{2/3} - 2.81\ (n-\tfrac{1}{4})^{2/3} \tag{15}$$

where h and h_T are in km and f in kHz.

Similarly for t_{n-z}, we can write:

$$(t_{n-z}) = 5.15 \text{ X } 10^{-3}\ (h-h_R)f^{2/3} - 2.81\ (n-\tfrac{1}{4})^{2/3} \tag{16}$$

or

$$(t_{n-z}) = 3.72 \text{ X } 10^{-2}\ (h-hT) - 2.81\ (n-\tfrac{1}{4})^{2/3} \tag{15a}$$

for f = 19.4 kH

and

$$(t_{n-z}) = 4.64 \text{ X } 10^{-2}\ (h-h_T) - 2.81\ (n-\tfrac{1}{4})^{2/3} \tag{15b}$$

for f = 27 kHz

Similarly, for t_{n-z}, we can write:

$$(t_{n-z}) = 3.72 \text{ X } 10^{-2}\ (h-h_T) - 2.81\ (n-\tfrac{1}{4})^{2/3} \tag{16a}$$

for f = 19.4 kHz

and

$$(t_{n-z}) = 4.64 \text{ X } 10^{-2}\ (h-h_T) - 2.81\ (n-\tfrac{1}{4})^{2/3} \tag{16b}$$

for f = 27 kHz

Using equations (12), (15) and (16) in equation (11) we can develop the expression for HGF in a simplified form as follows:

$$HGF = h \left(\frac{4\Pi^4}{6aC^2}\right)^{1/3} \left(n-\frac{1}{4}\right)^{-1/3} f^{2/3}$$

$$X \left[A_i\left(\frac{2}{a}\left(\frac{\Pi a}{c}\right)^{2/3} f^{2/3}(h-h_T) - 2.83 \left(n-\frac{1}{4}\right)^{2/3}\right)\right]$$

$$X \left[A_i\left(\frac{2}{a}\left(\frac{\Pi a}{c}\right)^{2/3} f^{2/3}(h-h_R) - 2.83 \left(n-\frac{1}{4}\right)^{2/3}\right)\right]$$

or

$$HGF = 3.49 \times 10^{-2} h \left(n-\frac{1}{4}\right)^{-1/3}$$

$$X \; A_i\left(3.72 \times 10^{-2}(h-h_T) - 2.81 \left(n-\frac{1}{4}\right)^{2/3}\right)$$

$$X \; A \left(3.72 \times 10^{-2}(h-h_R) - 2.81 \left(n-\frac{1}{4}\right)^{2/3}\right)$$

for f = 19.4 kHz (17)

and

$$HGF = 4.35 \times 10^{-2} \; h\left(n-\frac{1}{4}\right)^{-1/3} \times A_i\left(4.64 \times 10^{-2}(h-h_T) - 2.81\left(n-\frac{1}{4}\right)^{2/3}\right)$$

$$\times A_i\left(4.64 \times 10^{-2} \; (h-h_R) - 2.81 \; \left(n-\frac{1}{4}\right)^{2/3}\right) \quad (18)$$

for f = 27 kHz

Tabulated values of Airy functions, A, for different values of their arguments as obtained for various values of h_T and h_R, the heights of the transmitting and receiving antennas, are listed in Table I. The values have been obtained from reference (8). The appropriate values of α(dB/Mm), the attenuation constant, for different modes (mode 1 through 3), and for day and night time conditions are given in Table II. These values were obtained from reference (1).

From the values given in this table, it is found that the attenuation rate for the first order mode is less at the lower frequency during the daytime and increases during the nighttime. On the contrary, for the second and third order modes, the attenuation constant decreases during the nighttime. The trend is the same for the higher frequency (27 kHz).

Using the values of Airy functions for various augments as listed in Table II, the corresponding values of modified height gain factors for all the modes (mode 1 through 3) have been calculated for the condition when the receiving and transmitting antennas are at the same elevation. The controlling parameters are the transmitting/receiving antenna elevation, the propagation condition for the ionosphere, and the transmission frequency. The numerical values are given in Table II and shown in graphical form in Figures 1 and 2. The calculations have also been repeated for the condition when the receiving antenna is ground-based and the elevation of the transmitting antenna is increased above the ground. These tabulated values are given in Table III and the graphical forms have been represented in Figures 3 and 4. It should be emphasized at this point that these values of the modified height gain factors along with the corresponding values of the attenuation constant determine the values of the vertical component of the individual and multimode field strength as a function of distance and the resultant model interference pattern.

With these calculated values of α and HGF's, the amplitude of the vertical component of the field strength for any of the modes (mode 1 through 3), for any frequency (either 19.4 or 27 kHz) and for any propagation condition of the ionosphere (h=70 km for the daytime condition and h=90 km for the nighttime condition) can be computed by using the Equations 7 through 10.

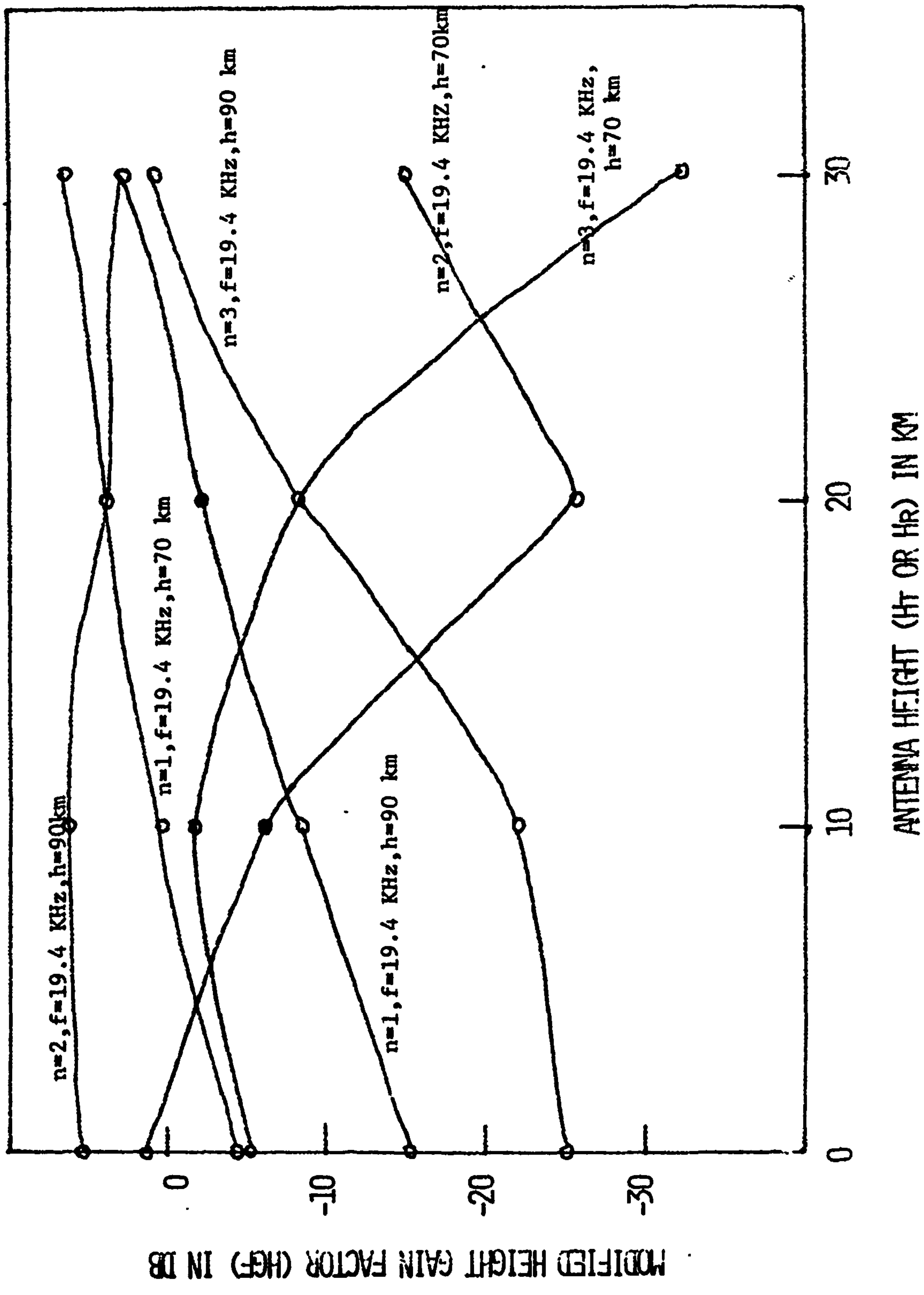

FIGURE 1. MODIFIED HEIGHT GAIN FACTOR VS ANTENNA HEIGHT ($H_T = H_R$, F = 19.4 KHZ)

FIGURE 2. MODIFIED HEIGHT GAIN FUNCTION VS ANTENNA HEIGHT ($H_T = H_R$, F = 27 KHZ)

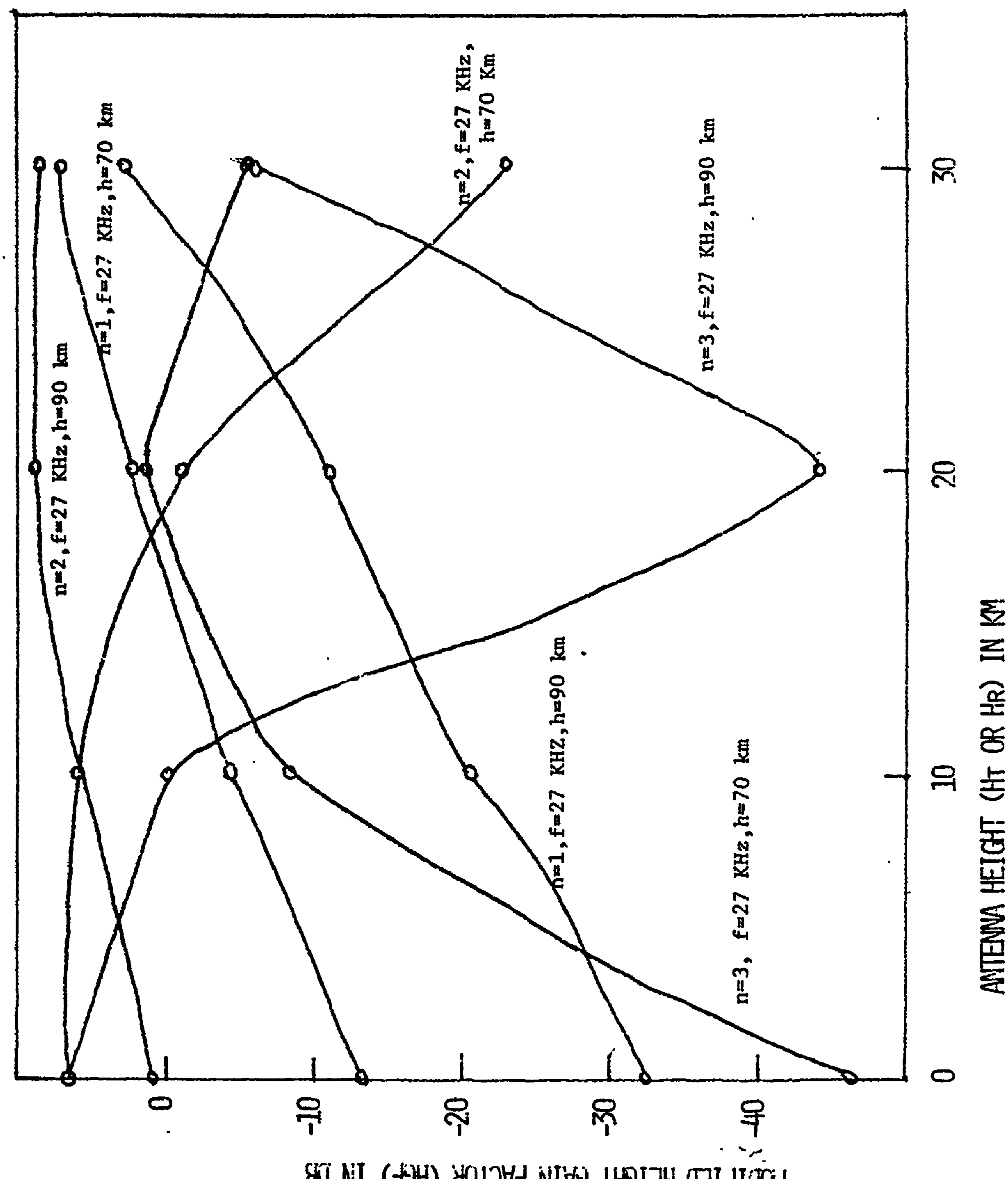

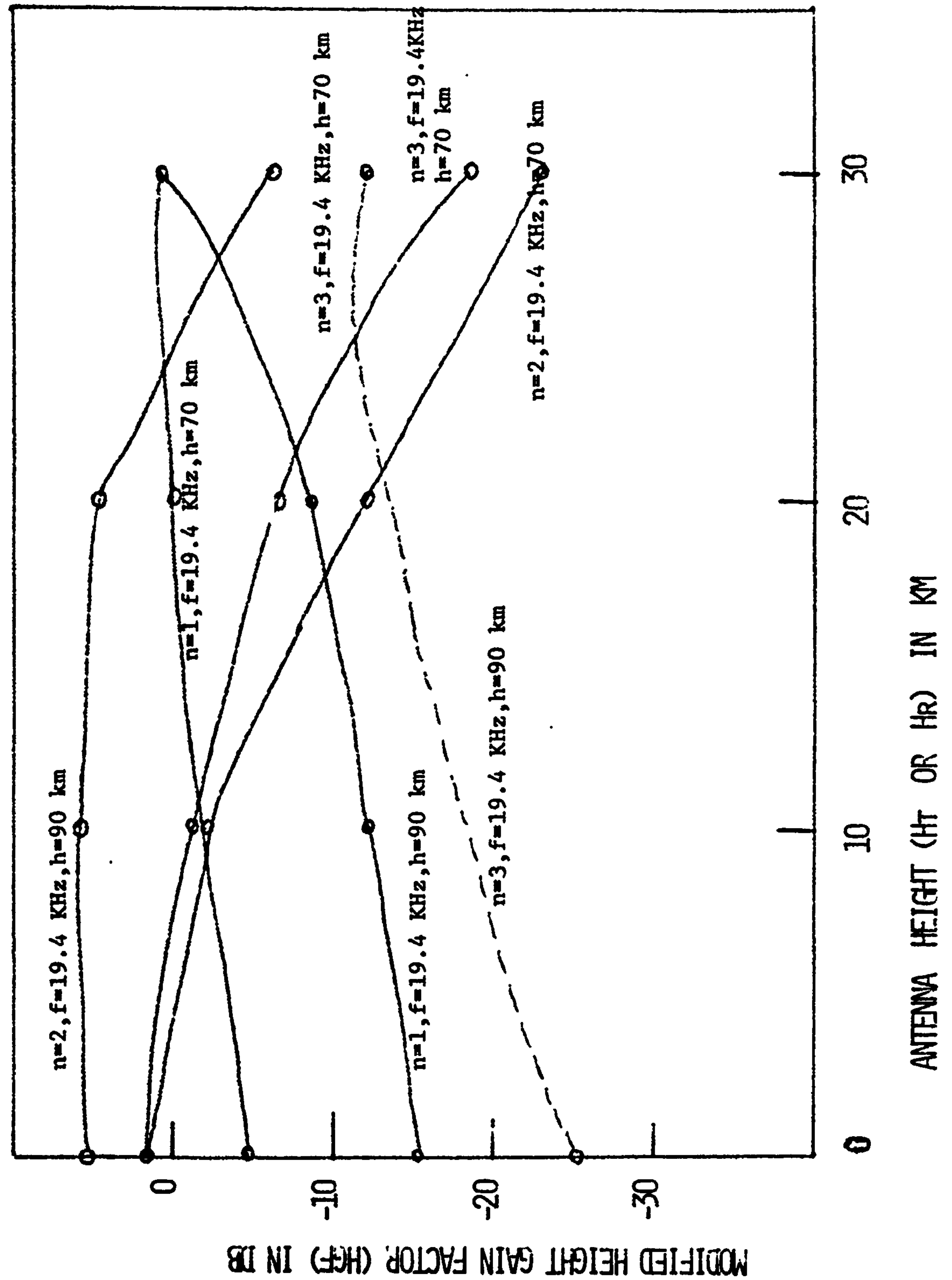

FIGURE 3. MODIFIED HEIGHT GAIN FUNCTION VS ANTENNA HEIGHT. (HR = 0., F=19.4 KHZ)

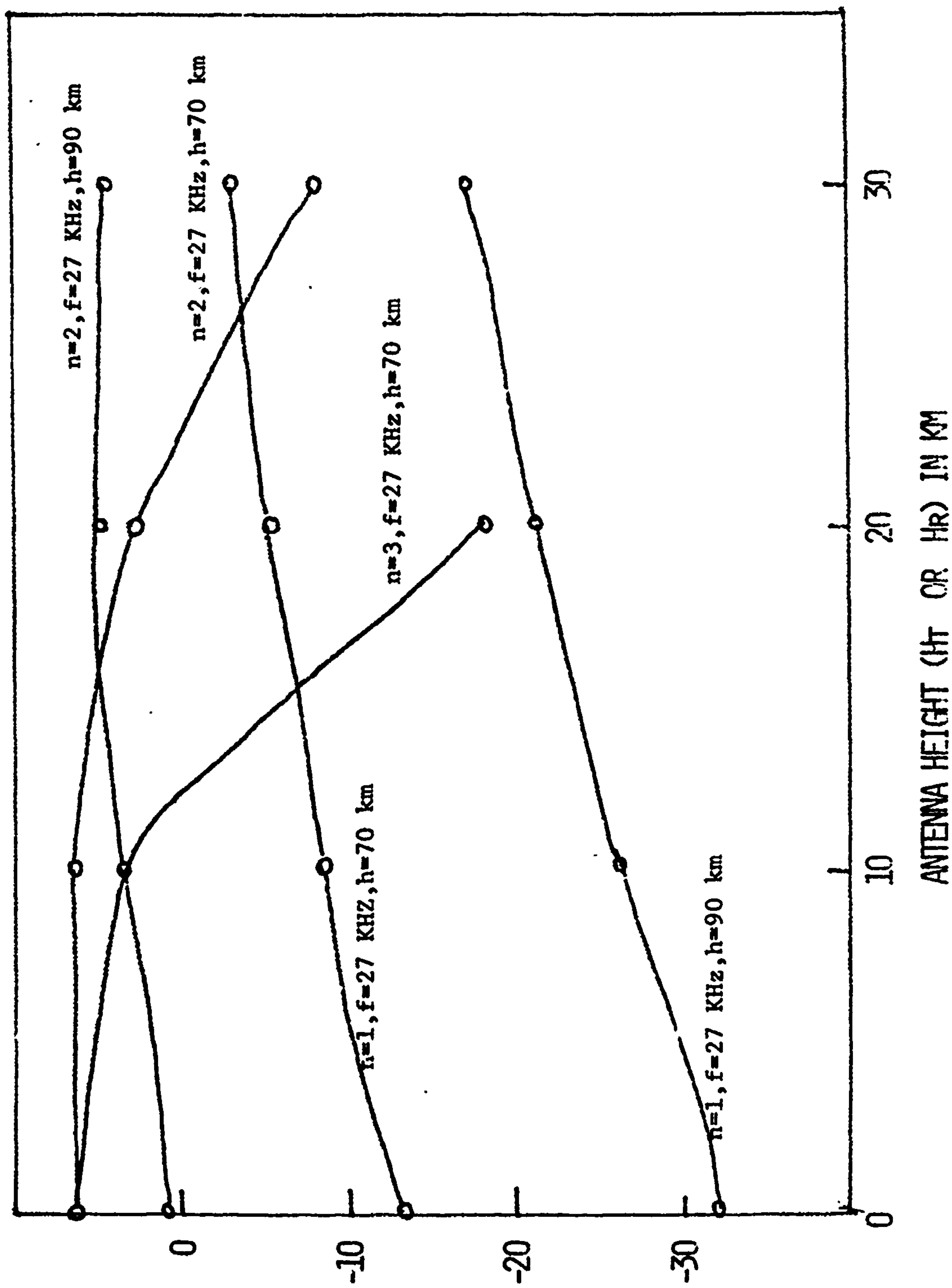

FIGURE 4. MODIFIED HEIGHT GAIN FACTOR VS ANTENNA HEIGHT (HR=0, F=27 KHZ)

TABLE I. VALUE OF σ, AN AUXILIARY VARIABLE

f (kHz)	h (km)	n	α (dB/Mm)	$\sigma = 4.83 \times 10^{-3}\, h\, f^{2/3} (n - \frac{1}{4})^{-1/3}$
19.4	70	1	1.56	7.2193
		2	6.56	5.443
		3	15.19	4.682
	90	1	1.62	9.282
		2	3.20	6.998
		3	7.80	6.019
27	70	1	2.00	10.047
		2	4.54	7.575
		3	10.54	6.516
	90	1	2.48	12.918
		2	2.30	9.740
		3	5.56	8.377

TABLE II. VALUES OF MODIFIED HEIGHT GAIN FACTORS ($h_T = h_R$)

f (kHz)	h (km)	h_T (km)	n	$t_n - z$	Ai ($t_n - z$)	HGF (dB)
19.4	70	0	1	0.2844	0.2837	- 4.72
			2	-1.4767	0.4643	1.39
			3	-2.9116	-0.3419	- 5.24
		10	1	-0.0876	0.3783	0.28
			2	-1.8487	0.3008	- 6.15
			3	-3.2836	-0.4172	- 1.78
		20	1	-0.4596	0.4674	3.96
			2	-2.2207	0.0962	-25.96
			3	-3.6556	-0.282	- 8.58
		30	1	-0.8316	0.5266	6.03
			2	-2.5927	-0.1785	-15.22
			3	-4.0276	-0.0703	-32.71
	90	0	1	1.0284	0.1353	-15.4
			2	-0.7327	0.5152	5.38
			3	-2.1676	0.096	-25.12
		10	1	0.6564	0.1973	- 8.84
			2	-1.1047	0.5338	6.0
			3	-3.5396	-0.1123	-22.39
		20	1	0.2844	0.2834	- 2.55
			2	-1.4767	0.4643	3.57
			3	-2.9116	-0.3419	- 3.05
		30	1	-0.0876	0.3783	2.47
			2	-1.8487	0.2868	- 4.80
			3	-3.2836	0.4172	0.40
27	70	0	1	0.9284	0.1468	-13.29
			2	-0.8327	0.5266	6.45
			3	-2.2676	0.0267	-46.66
		10	1	0.4644	0.2408	- 4.69
			2	-1.2967	0.5123	5.97
			3	-2.7316	-0.2400	- 8.51
		20	1	3.9611×10^{-4}	0.3550	2.05
			2	-1.7607	0.3408	- 1.14
			3	-3.1956	-0.4175	1.11
		30	1	-0.4636	0.4674	6.83
			2	-2.2247	0.0961	-23.10
			3	-3.6596	-0.2820	- 5.71
	90	0	1	1.8564	0.0431	-32.40
			2	0.0953	0.3318	0.61
			3	-1.3396	0.5123	6.84

TABLE II (CONTINUED)

f (kHz)	h (km)	h_T (km)	n	$t_n - z$	$Ai(t_n - z)$	HGF (dB)
27	90	10	1	1.3924	0.0834	-20.93
			2	-0.3687	0.4474	5.80
			3	-1.8036	0.3408	- 0.24
		20	1	0.9284	0.1468	-11.11
			2	-0.8327	0.5266	8.63
			3	-2.2676	0.0267	-44.48
		30	1	0.4644	0.2408	2.51
			2	-1.2967	0.5123	8.15
			3	-2.7316	-0.2400	- 6.33

TABLE III. VALUES OF MODIFIED HEIGHT GAIN FACTORS ($h_R \neq h_T$)

f (kHz)	h (km)	h_R (km)	h_T (km)	n	HGF (dB)
19.4	70	0	0	1	- 4.72
				2	1.39
				3	- 5.24
			10	1	- 2.22
				2	- 2.38
				3	- 3.51
			20	1	- 0.38
				2	-12.27
				3	- 6.91
			30	1	0.66
				2	-23.42
				3	-18.98
	90	0	0	1	-15.40
				2	5.38
				3	-25.12
			10	1	-12.12
				2	5.69
				3	
			20	1	- 8.97
				2	4.48
				3	
			30	1	- 6.47
				2	0.29
				3	-12.35
27	70	0	0	1	-13.29
				2	6.45
				3	-46.66
			10	1	- 8.99
				2	6.21
				3	
			20	1	- 5.62
				2	2.67
				3	
			30	1	- 3.23
				2	- 8.33
				3	

TABLE III (CONTINUED)

f (kHz)	h (km)	h_R (km)	h_T (km)	n	HGF (dB)
27	90	0	0	1	-32.40
				2	0.61
				3	6.84
			10	1	-26.66
				2	3.20
				3	3.30
			20	1	-21.75
				2	4.62
				3	-18.82
			30	1	-17.45
				2	4.38
				3	

MULTIMODE FIELD STRENGTHS

At long distances the field strengths due to second and third order mode are equally important. Hence, total field strengths at large distances are the vector sum of individual mode field components. To calculate such resultant field strength, a knowledge of the phase of the individual mode at a certain distance is essential.

The phase of the vertical component of the nth mode (n = 1,or 2 or 3) field strength with respect to the transmitting antenna current is given by equation (4) as

$$\phi_{E_{z,n}} = \frac{\pi}{4} - \omega D / v_{p,n} + \phi_{\Lambda_n}$$

$$= \frac{\pi}{4} - \frac{2\pi \; Dc}{\lambda \; v_{p,n}} + \phi_{\Lambda_n}$$

where c is the speed of light in free space and the other terms have their previously defined meanings. The values of $c/v_{p,n}$ and $\phi_{\Lambda n}$, as obtained from reference (1),are given in Table III. With the values of $c/v_{p,n}$ and $\phi_{\Lambda n}$, values of $\phi_{E_{z,n}}$ for any mode, the frequency, distance and ionospheric conditions can be calculated from the equation cited above. The values of $\phi_{E_{z,n}}$ thus calculated for different modes and frequencies are listed in Table IV. From this table, it is also found that the difference in phase between first and second order modes for f = 19.4 kHz is

$$\Delta \phi_{1,2} = 5.01 \text{ radian/Mm during daytime (h =70 km)}$$

$$= 3.20 \text{ radian/Mm during nighttime (h =90 km)}$$

and for f = 27 kHz

$$\Delta \phi_{1,2} = 4.22 \text{ radian/Mm during daytime (h=70 km)}$$

$$2.33 \text{ radian/Mm during nighttime (h=90 km)}$$

Furthermore, with known values of $_{E_{z,n}}$, the amplitude of the vertical component of the multimode field strength is calculated as follows:

$$E = \left((E_{z1} \cos \phi_{E_{z1}} + E_{z2} \cos \phi_{E_{z2}} + E_{z3} \cos \phi_{E_{z3}})^2 \right.$$
$$\left. (E_{z1} \sin \phi_{E_{z1}} + E_{z2} \sin \phi_{E_{z2}} + E_{z3} \sin \phi_{E_{z3}})^2 \right)^{1/2}$$

TABLE IV. - VALUES FOR ϕ^{o}_{n}, $\frac{\nu_{pn}}{c}$ AND ϕn

f (kHz)	h (km)	n	ϕ^{o}_{n}	$\frac{\nu_{pn}}{c}$	ϕn
19.4	70	1	7.50	0.9984	0.916-0.407D
		2	1.40	1.011	0.809-0.402D
		3	0.78	1.042	0.799-0.390D
	90	1	13.12	0.996	1.014-0.408D
		2	1.82	1.0038	0.817-0.405D
		3	0.66	1.02	0.797-0.398D
27	70	1	14.2	0.997	1.033-0.567D
		2	1.6	1.0035	0.813-0.563D
		3	0.42	1.017	0.792-0.556D
	90	1	25.5	0.9944	1.23-0.568D
		2	6.5	0.9994	0.898-0.566D
		3	-0.03	1.0065	0.785-0.562D

ϕ is calculated from

$$\phi = \frac{\pi}{4} - \frac{\omega D}{\nu} + \phi_n \quad \text{rad}$$

$$= \frac{\pi}{4} - \frac{2}{\lambda} D \frac{c}{\nu_{pn}} + \phi_n$$

where λ, D in km, $\lambda - \frac{300}{f}$, f in kHz.

and the corresponding phase is calculated from

$$\phi = \tan^{-1}\left(\frac{E_{z1}\sin\phi_{Ez1} + E_{z2}\sin\phi_{Ez2} + E_{z3}\sin\phi_{Ez3}}{E_{z1}\cos\phi_{Ez1} + E_{z2}\cos\phi_{Ez2} + E_{z3}\cos\phi_{Ez3}}\right) \tag{20}$$

DISCUSSION

A microcomputer (Tektronix 4054 with accompanying Hard Copy Unit 4631) was used for all the computational works reported in this report. A computer program written in BASIC and provided in Appendix A has been used to compute the values of E_{zn}, the vertical component of the individual mode electric field strength as a function of distance based on any of the Equations 7 through 10. The sample program shown in Appendix B was used for the computation of the values of E_z, the multimode field strength based on Equation 19 and provides the output in graphical and tabular forms. These graphical plots have been represented in Figures 5 through 20. For all these plots, the transmitting and receiving antennas are assumed to be at the same elevation and the controlling parameters use either the frequency, the height of the ionospheric reflection point, or the elevation of the transmitting/receiving antennas. Distances are varied up to 3000 km and the elevation of the transmitting/receiving antennas up to 30 km in order to conform to the plans of the experiment. Figures 21 through 32 illustrate similar results when the receiving antenna is ground-based and the transmitting antenna elevation is varied up to 30 km in steps of 10 km.

The signature of strong interference phenomenon due to individual modes on the modesum field strength is apparent and it is indicative of the fact that at many locations, although the individual mode field strength is strong, the modesum field strength is relatively weak due to modal interference. At low frequency (19.4 kHz) and during daytime, the interference pattern begins to appear at short distances. For the ground-based transmitting and receiving antennas, the modesum field strength curve displays strong interference pattern with bit nulls occurring at 600 km and 2000 km as can be seen in Figure 5. The interference phenomenon becomes weaker as the antenna elevation is increased and at an antenna height around 30 km it disappears completely as is seen in Figure 8. This variation of interference phenomenon can be attributed to the fact that at higher altitude, the height gain factor for the first order mode increases and for the second and third order mode it decreases. Furthermore, the attenuation constant for the first order mode is very low (1.5 dB/Mm) whereas for the second and third order modes attenuation constant is fairly high (5.6 dB/Mm and 15.2 dB/Mm). All these factors combine together to make the field strength curve for the first order mode predominant at large distances thereby making the interference pattern very weak.

Interference patterns during nighttime are illustrated in Figures 9 through 12. It is seen in these figures that at nighttime, the interference phenomenon is very weak when the antenna elevation is low and gets stronger as the elevation is increased and is strongest when the antenna height is 30 km. A prominent null occurs at 1000 km as is seen in Figure 12. Referring to Figure 1, it is found that at nighttime the attenuation rate for the first order mode is higher than during the daytime whereas for the second and third order modes, this rate is lower. The height gain factor for the second order mode does not fall off fast with antenna elevation and for the third order mode it rather increases. The net effect of these factors is to make the second and third order mode field strengths very strong and results in a strong interference pattern for the multimode field strength curve.

At the higher frequency (27 kHz) and during the daytime propagation condition, a reverse condition for the interference is displayed by the multimode field strength curve as is shown in Figures 13 through 16. At lower antenna elevation, the second order mode curve is weak and the third order mode curve is weakest making the multimode interference phenomenon less prominent. As the antenna elevation increases, second and third order mode curves become stronger and a strong interference pattern is observed with a deep null occurring at 850 km when the transmitting and receiving antenna elevation is 20 km as is illustrated in Figure 15. As Figure 16 shows, above this height the interference phenomenon becomes weak.

Figures 17 through 20 show the interference pattern for the higher frequency (27 kHz) during the nighttime condition. For the ground-based antennas strong modal interference accompanied by two deep nulls occurs. The intensity of interference decreases as the transmitting/receiving antenna elevation is increased.

The interference phenomenon is also present in the multimode field strength curve as a function of distance both during the daytime and nighttime when the receiving antenna is ground-based and the transmitting antenna is elevated. The interference pattern changes from weak to strong and vice versa when this elevation is increased up to 30 km. As an example for the lower frequency, it is seen in Figure 21 that at closer distances and at lower antenna elevations, the height gain factors for the second and third order mode are fairly high making their corresponding field strengths strong. Interference phenomenon begins to appear at short distances, and a strong null occurs at 600 km. At higher transmitting antenna elevation, the interference pattern fades away as the second and third order mode fields become less predominant. At nighttime, the interference phenomenon is not so strong.

At higher frequency and during the daytime condition, the interference phenomenon is strong for the intermediate elevation of the transmitting antenna, the receiving antenna being ground-based and is characterized by the occurence of two strong nulls, one at 800 km and the other at 2400 km as are shown in Figure 24. During nighttime, a strong interference phenomenon occurs only when the transmitting antenna elevation is around 10 km. At higher elevations, the second and third order mode become less significant and the interference pattern disappears - making the multimode field strength curve equivalent to the first order mode field strength curve.

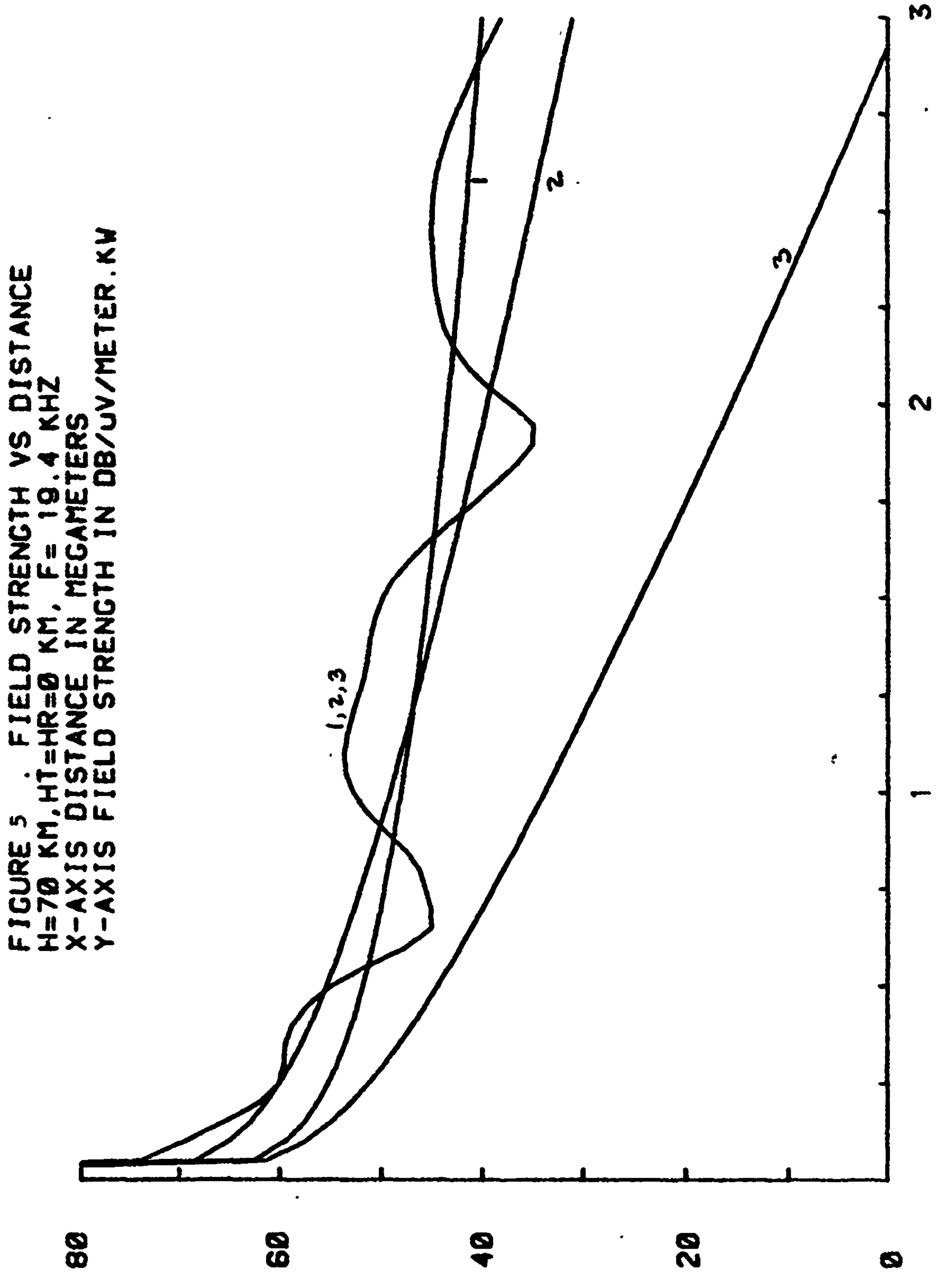

FIGURE 5 . FIELD STRENGTH VS DISTANCE
H=70 KM,HT=HR=0 KM, F= 19.4 KHZ
X-AXIS DISTANCE IN MEGAMETERS
Y-AXIS FIELD STRENGTH IN DB/uV/METER.KW

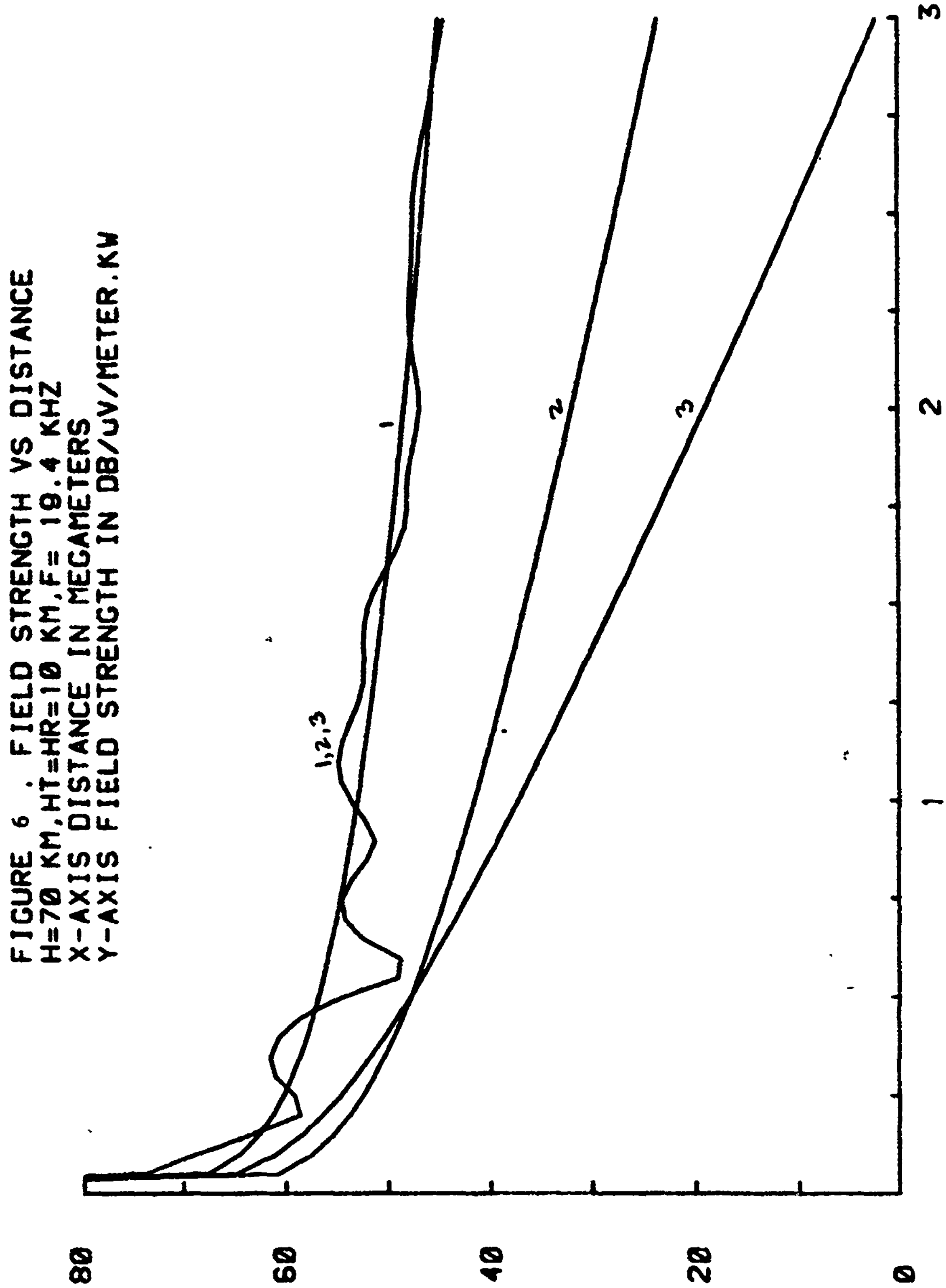

FIGURE 6 . FIELD STRENGTH VS DISTANCE
H=70 KM,HT=HR=10 KM,F= 19.4 KHZ
X-AXIS DISTANCE IN MEGAMETERS
Y-AXIS FIELD STRENGTH IN DB/UV/METER.KW

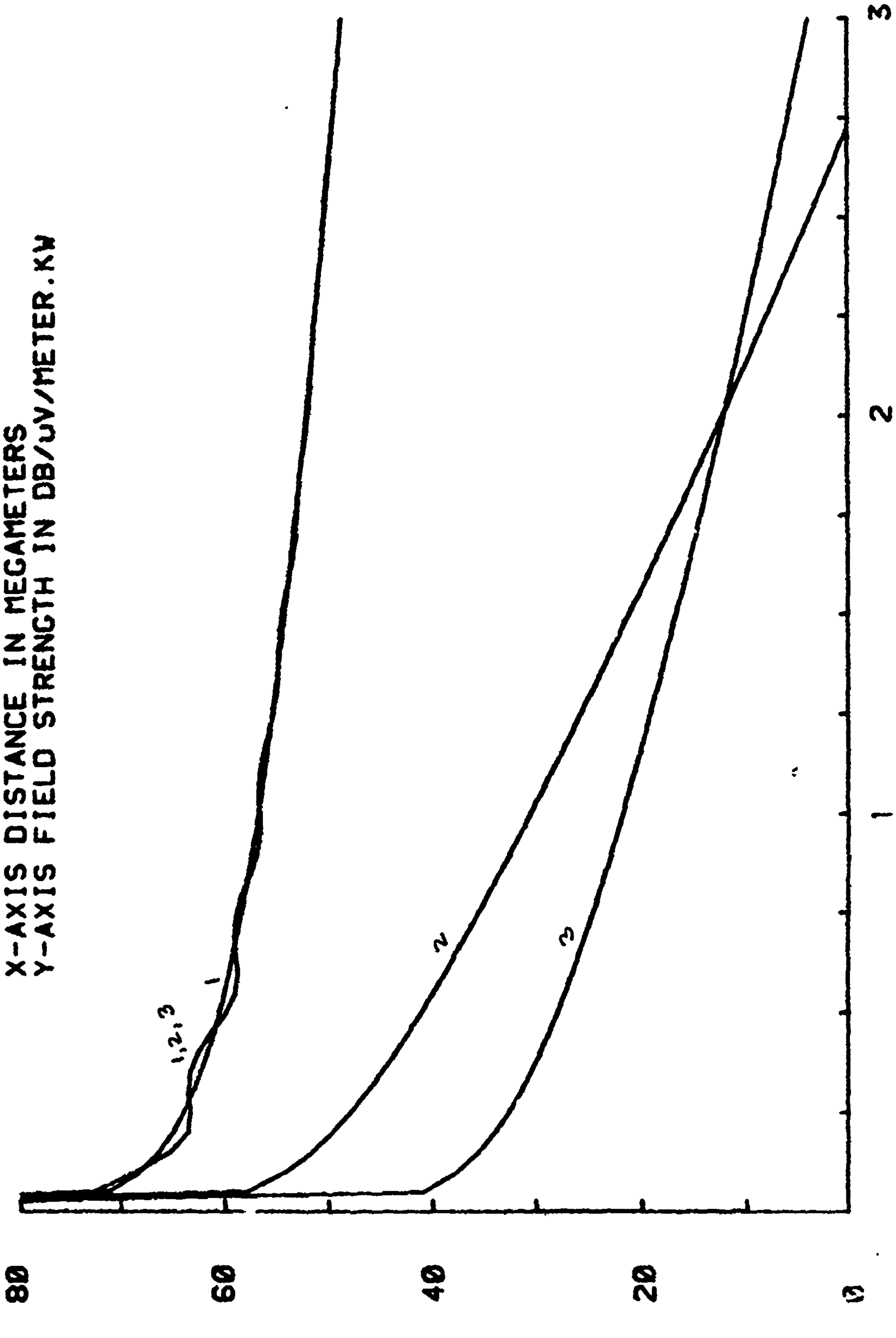

FIGURE 7 . FIELD STRENGTH VS DISTANCE
H=70 KM,HT=HR=20 KM,F= 19.4 KHZ
X-AXIS DISTANCE IN MEGAMETERS
Y-AXIS FIELD STRENGTH IN DB/uV/METER.KW

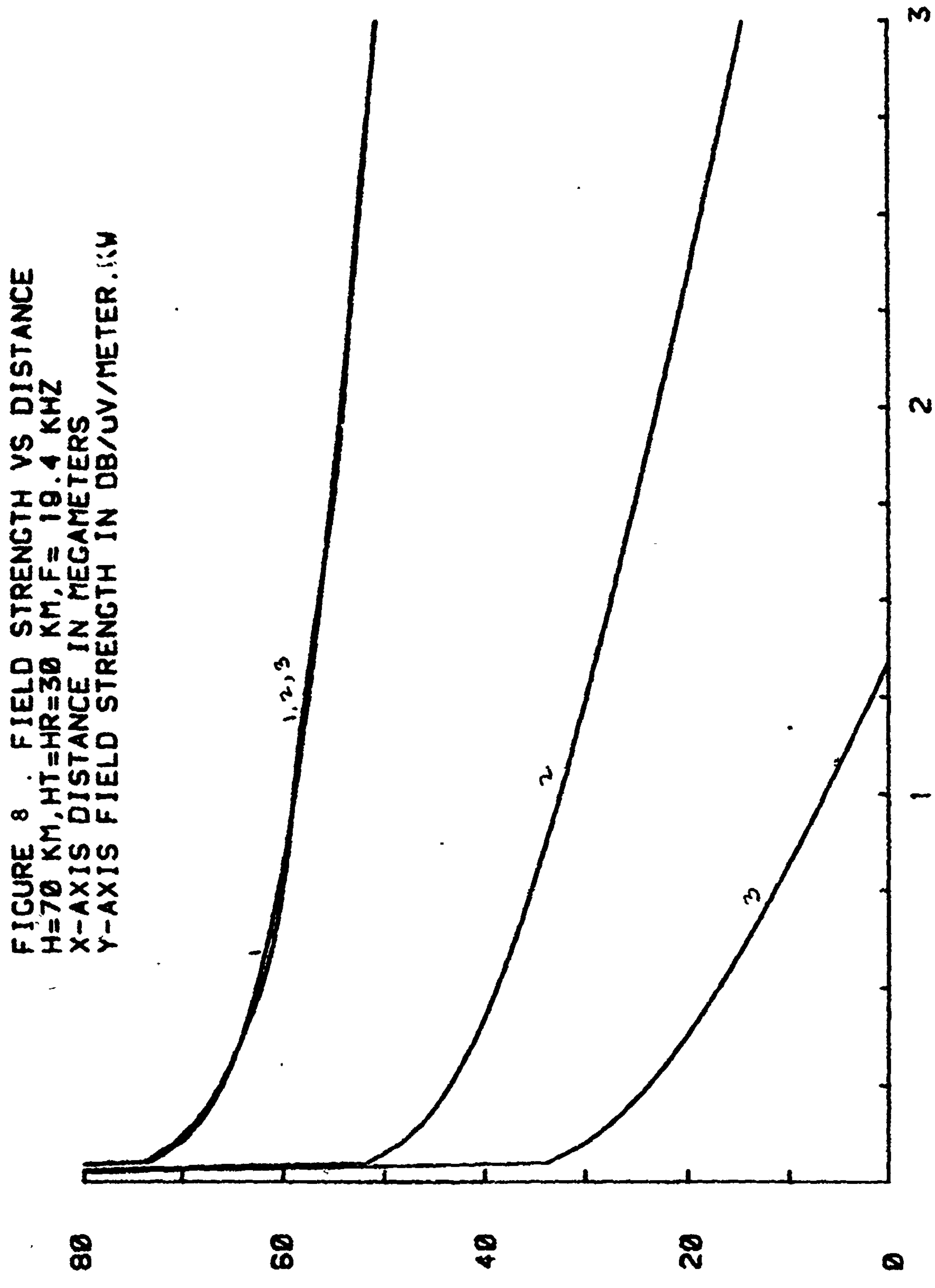
FIGURE 8 . FIELD STRENGTH VS DISTANCE
H=70 KM,HT=HR=30 KM,F= 19.4 KHZ
X-AXIS DISTANCE IN MEGAMETERS
Y-AXIS FIELD STRENGTH IN DB/UV/METER.KW
1,2,3
1
2
3
80
60
40
20
0
1
2
3

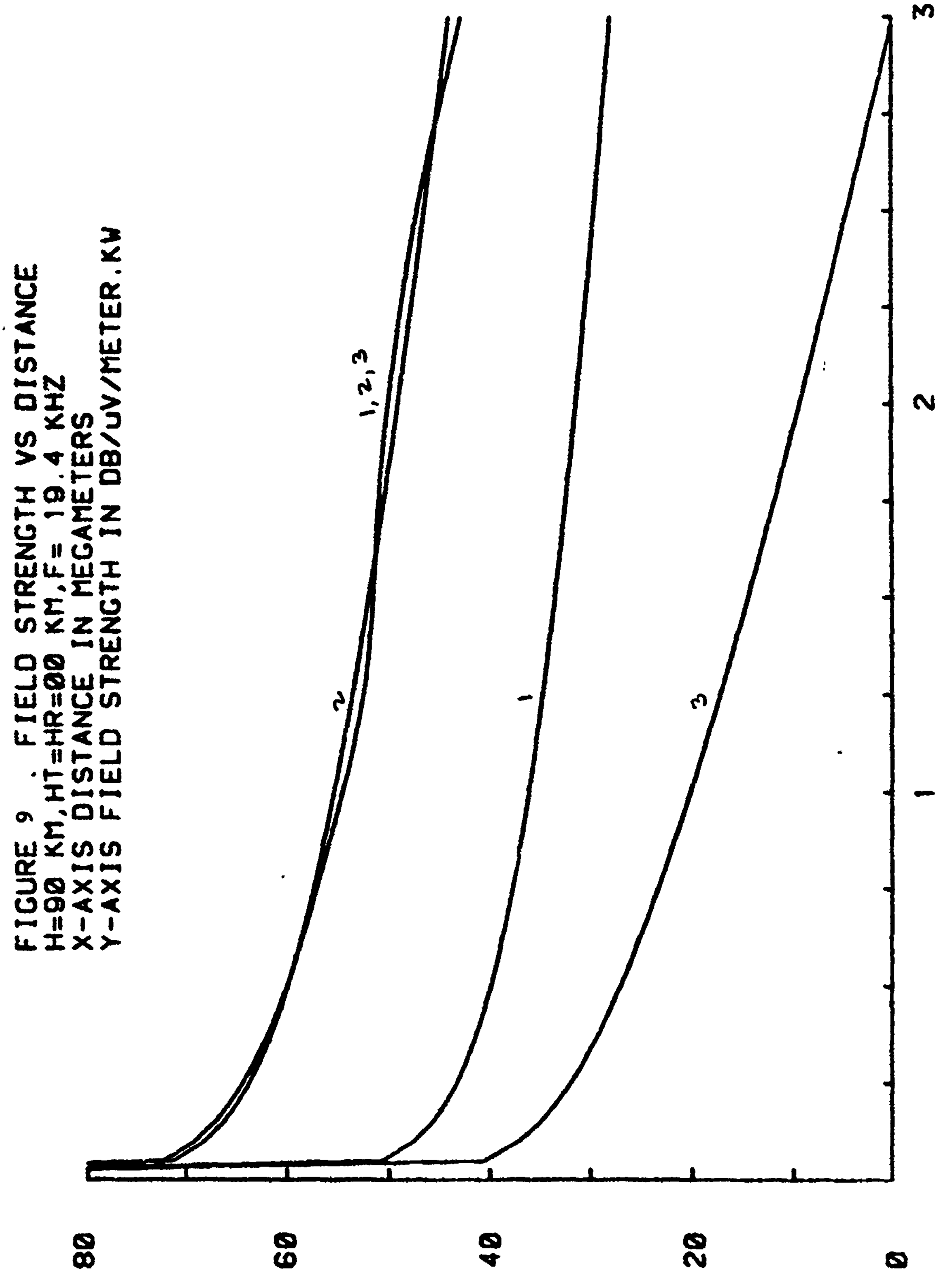

FIGURE 9 . FIELD STRENGTH VS DISTANCE
H=90 KM,HT=HR=00 KM,F= 19.4 KHZ
X-AXIS DISTANCE IN MEGAMETERS
Y-AXIS FIELD STRENGTH IN DB/uV/METER.KW

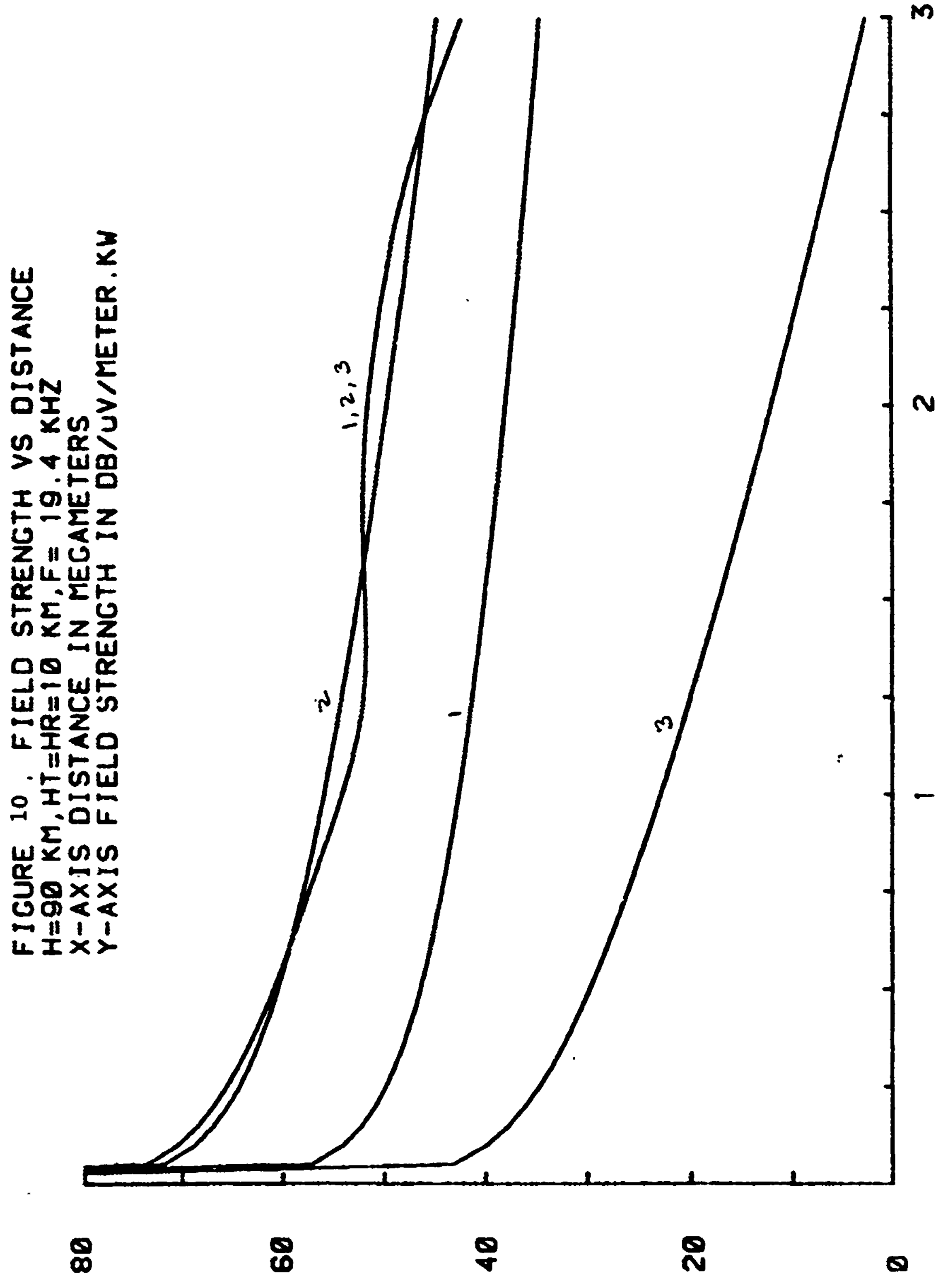

FIGURE 10. FIELD STRENGTH VS DISTANCE
H=90 KM,HT=HR=10 KM,F= 19.4 KHZ
X-AXIS DISTANCE IN MEGAMETERS
Y-AXIS FIELD STRENGTH IN DB/uV/METER.KW

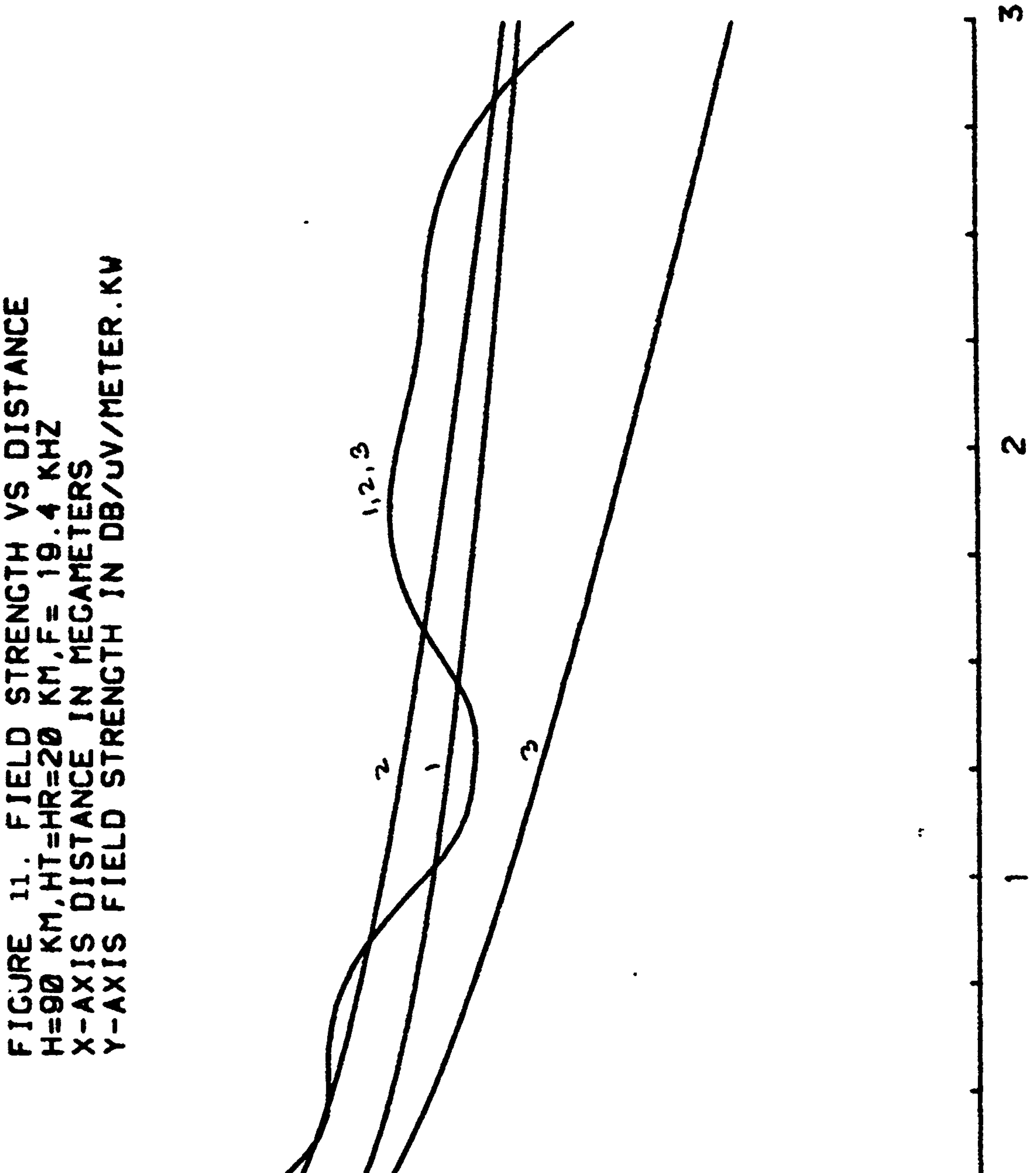

FIGURE 11. FIELD STRENGTH VS DISTANCE
H=90 KM,HT=HR=20 KM,F= 19.4 KHZ
X-AXIS DISTANCE IN MEGAMETERS
Y-AXIS FIELD STRENGTH IN DB/uV/METER.KW

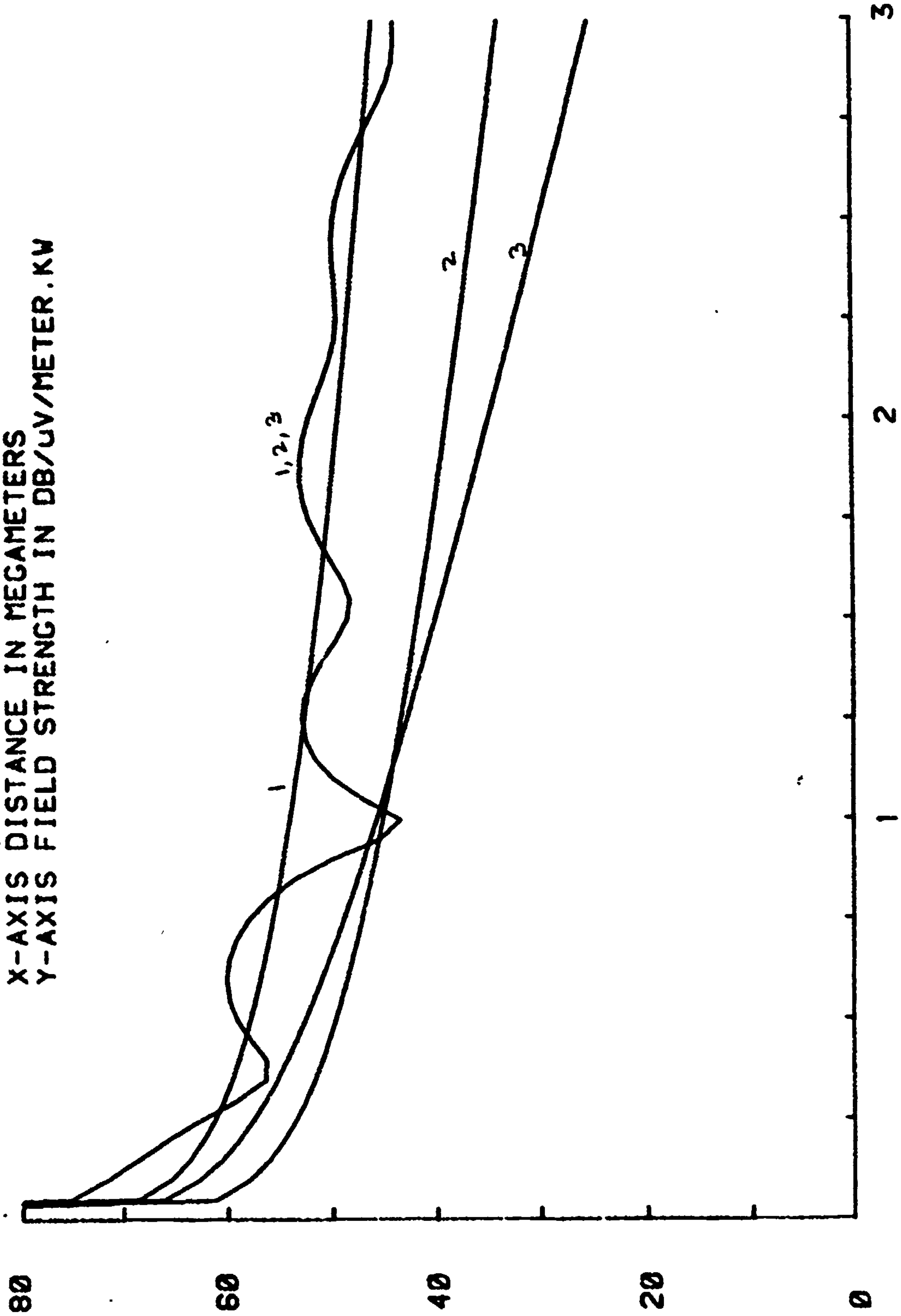

FIGURE 12 . FIELD STRENGTH VS DISTANCE
H=90 KM,HT=HR=30 KM,F= 19.4 KHZ
X-AXIS DISTANCE IN MEGAMETERS
Y-AXIS FIELD STRENGTH IN DB/uV/METER.KW

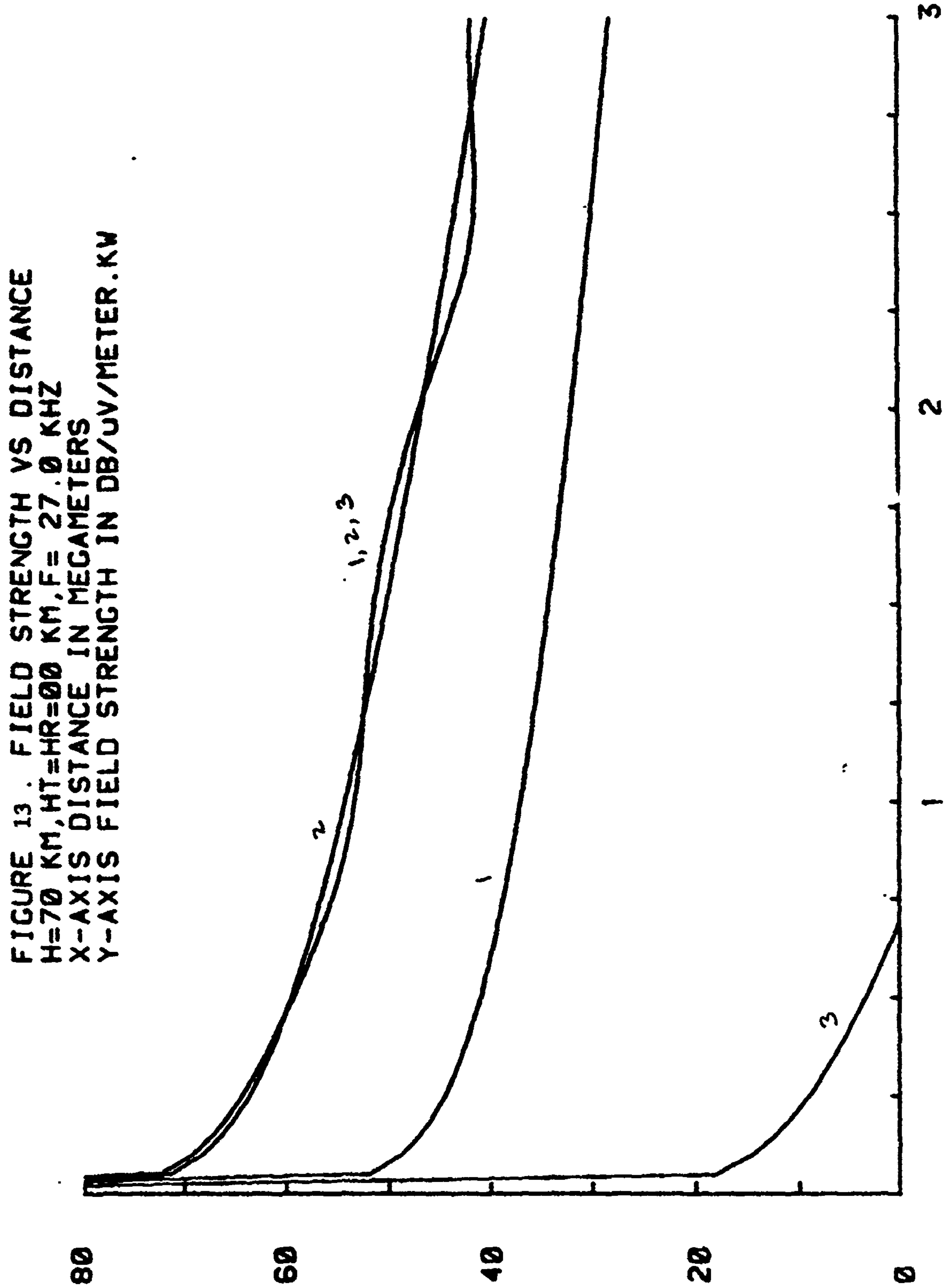

FIGURE 13 . FIELD STRENGTH VS DISTANCE
H=70 KM,HT=HR=00 KM,F= 27.0 KHZ
X-AXIS DISTANCE IN MEGAMETERS
Y-AXIS FIELD STRENGTH IN DB/UV/METER.KW

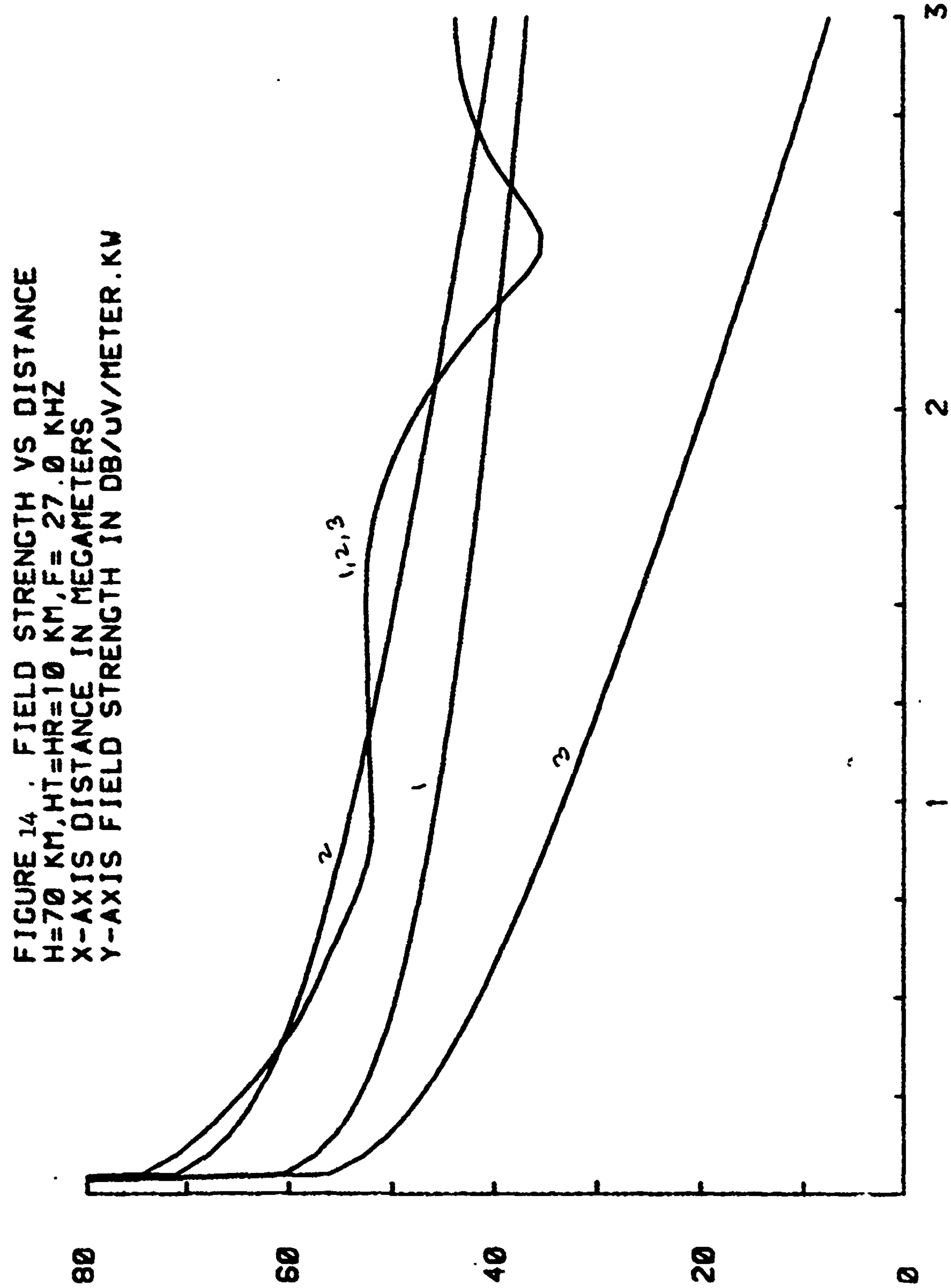

FIGURE 14 . FIELD STRENGTH VS DISTANCE
H=70 KM,HT=HR=10 KM,F= 27.0 KHZ
X-AXIS DISTANCE IN MEGAMETERS
Y-AXIS FIELD STRENGTH IN DB/UV/METER.KW

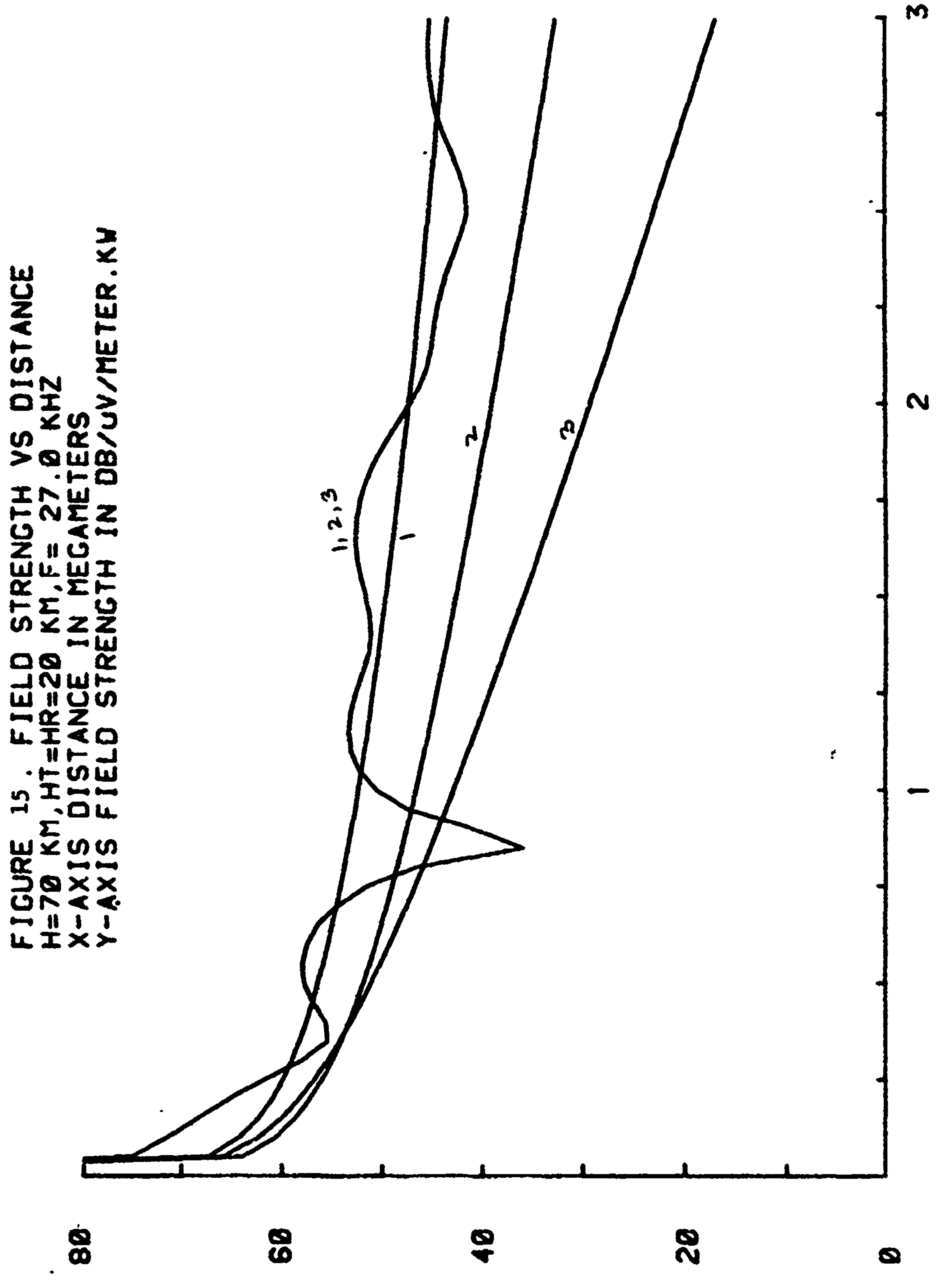

FIGURE 15. FIELD STRENGTH VS DISTANCE
H=70 KM,HT=HR=20 KM,F= 27.0 KHZ
X-AXIS DISTANCE IN MEGAMETERS
Y-AXIS FIELD STRENGTH IN DB/uV/METER.KW

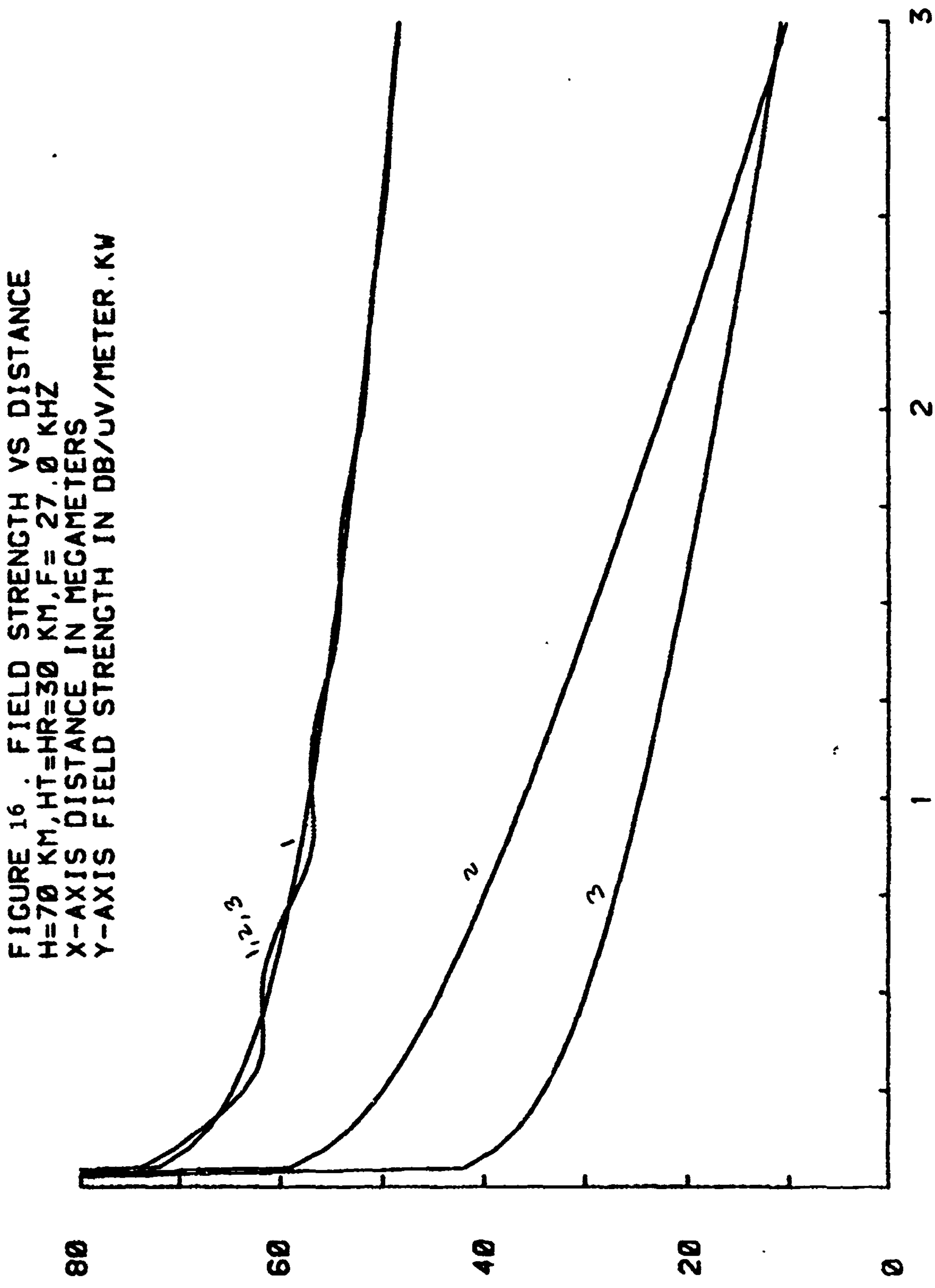
FIGURE 16 . FIELD STRENGTH VS DISTANCE
H=70 KM,HT=HR=30 KM,F= 27.0 KHZ
X-AXIS DISTANCE IN MEGAMETERS
Y-AXIS FIELD STRENGTH IN DB/UV/METER.KW
1,2,3
1
2
3
80
60
40
20
0
1
2
3

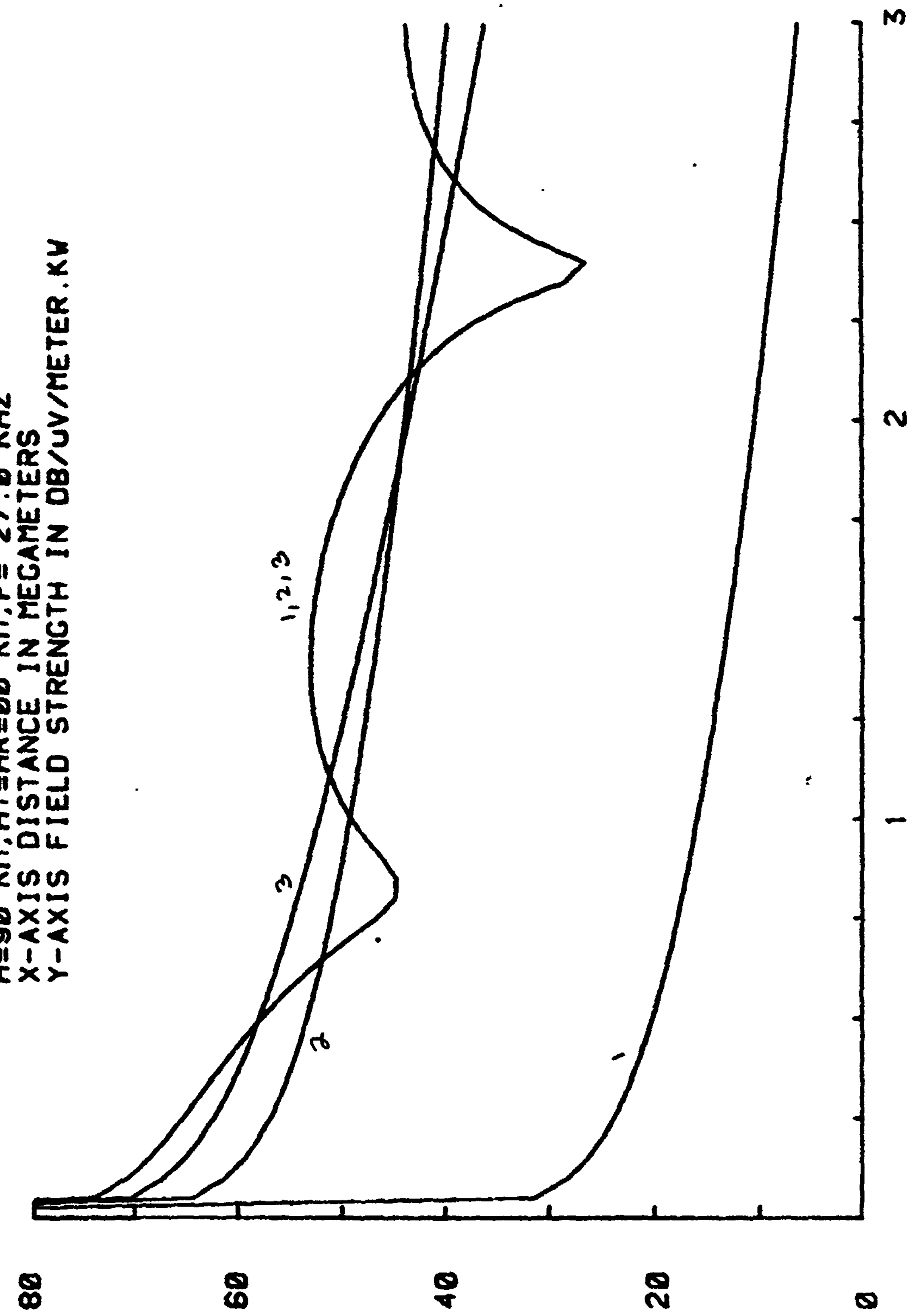

FIGURE 17 . FIELD STRENGTH VS DISTANCE
H=90 KM,HT=HR=00 KM,F= 27.0 KHZ
X-AXIS DISTANCE IN MEGAMETERS
Y-AXIS FIELD STRENGTH IN DB/UV/METER.KW

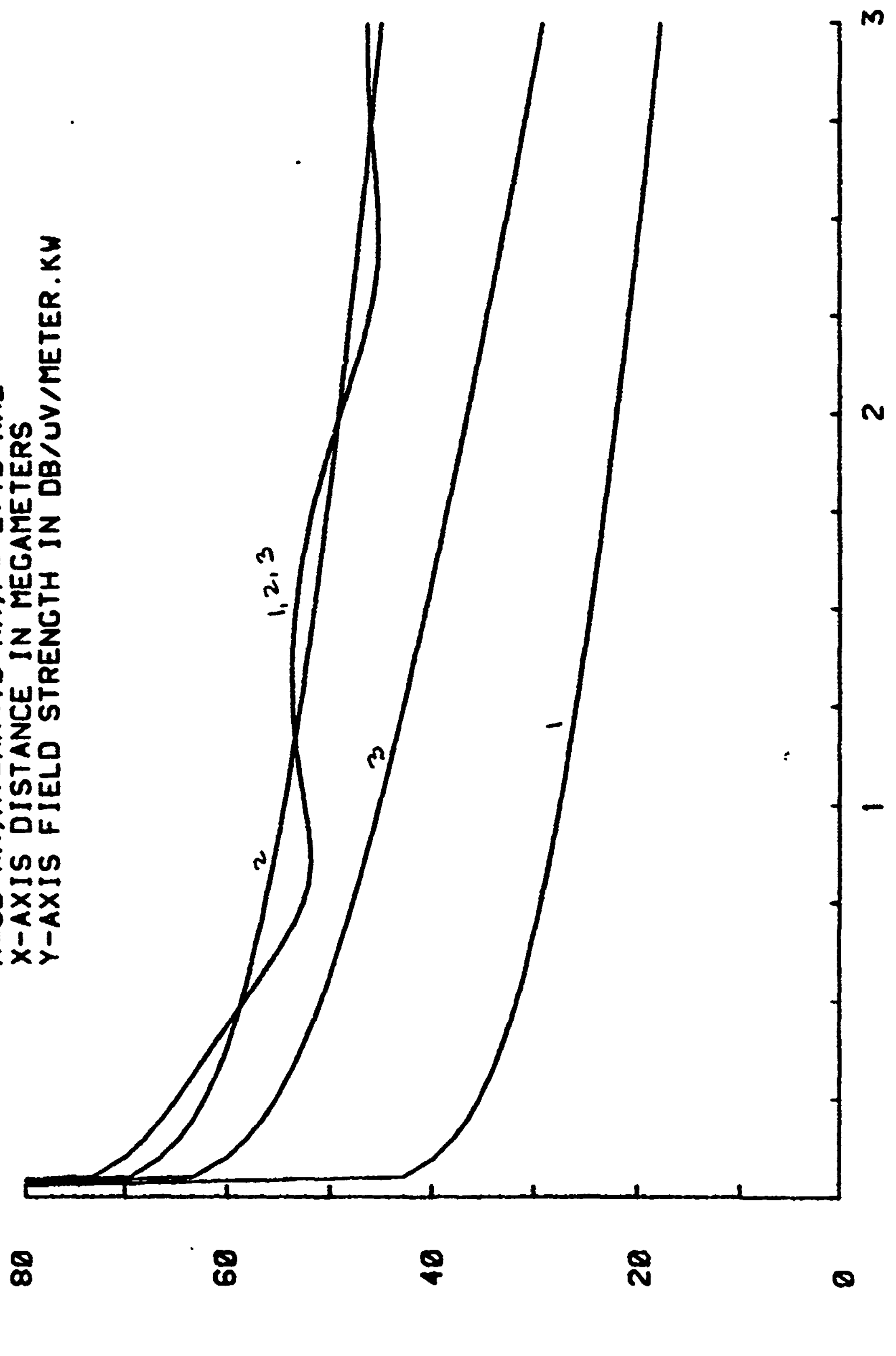

FIGURE 18 . FIELD STRENGTH VS DISTANCE
H=90 KM,HT=HR=10 KM,F= 27.0 KHZ
X-AXIS DISTANCE IN MEGAMETERS
Y-AXIS FIELD STRENGTH IN DB/uV/METER.KW

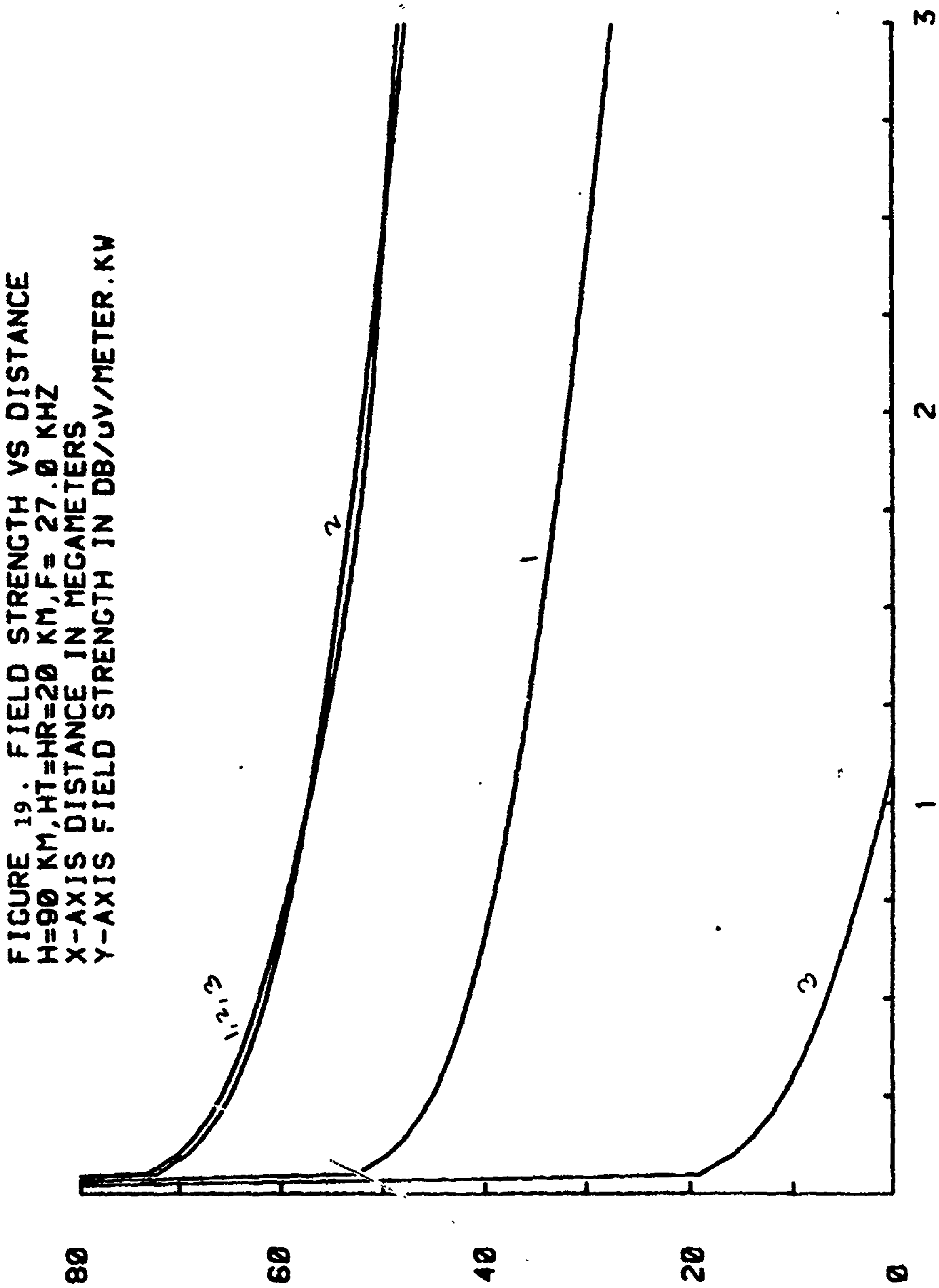
FIGURE 19. FIELD STRENGTH VS DISTANCE
H=90 KM,HT=HR=20 KM,F= 27.0 KHZ
X-AXIS DISTANCE IN MEGAMETERS
Y-AXIS FIELD STRENGTH IN DB/uV/METER.KW
80
60
40
20
0
1
2
3
1,2,3
2
1
3

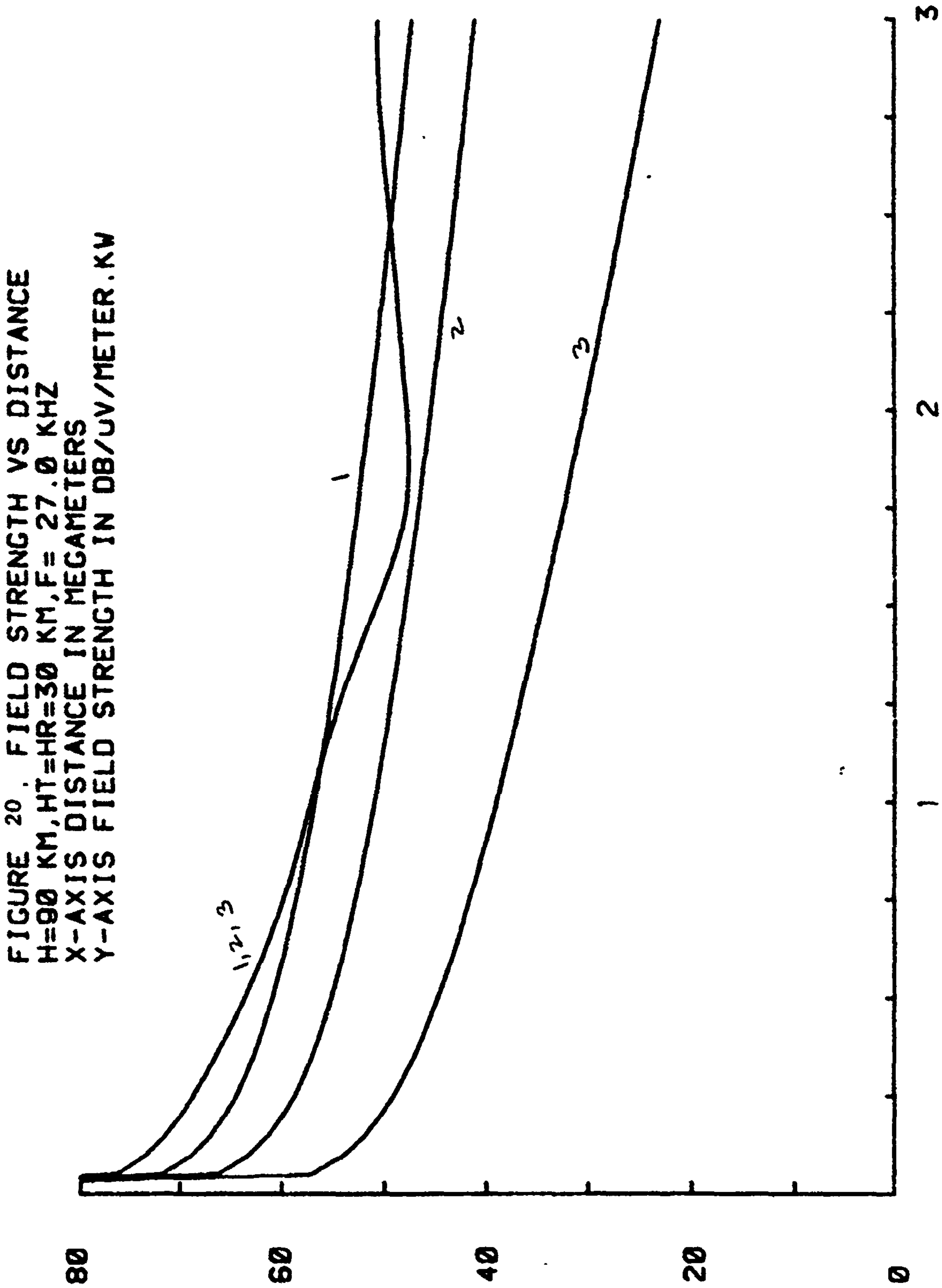

FIGURE 20. FIELD STRENGTH VS DISTANCE
H=90 KM,HT=HR=30 KM,F= 27.0 KHZ
X-AXIS DISTANCE IN MEGAMETERS
Y-AXIS FIELD STRENGTH IN DB/UV/METER.KW

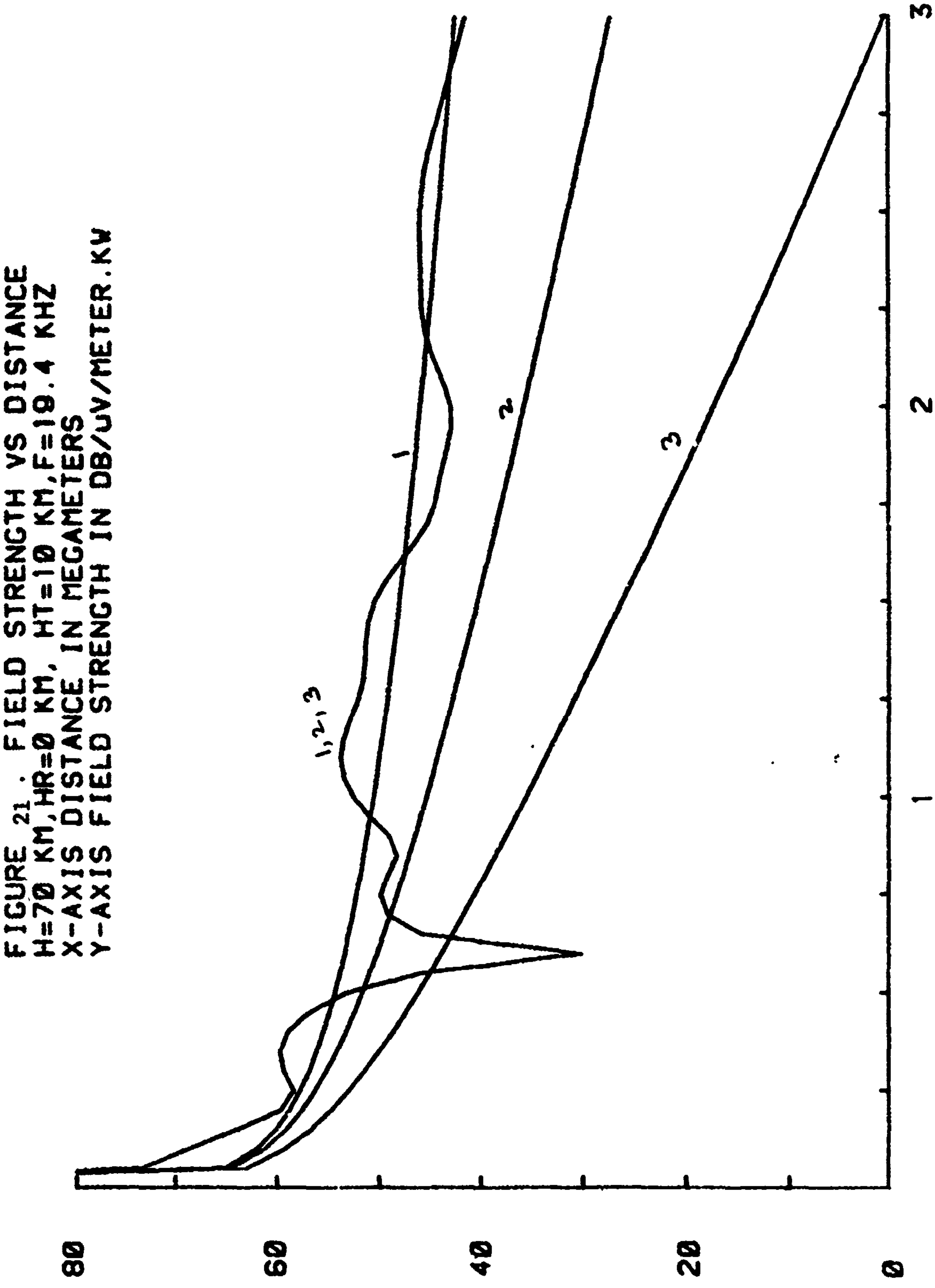

FIGURE 21. FIELD STRENGTH VS DISTANCE
H=70 KM,HR=0 KM, HT=10 KM,F=19.4 KHZ
X-AXIS DISTANCE IN MEGAMETERS
Y-AXIS FIELD STRENGTH IN DB/UV/METER.KW

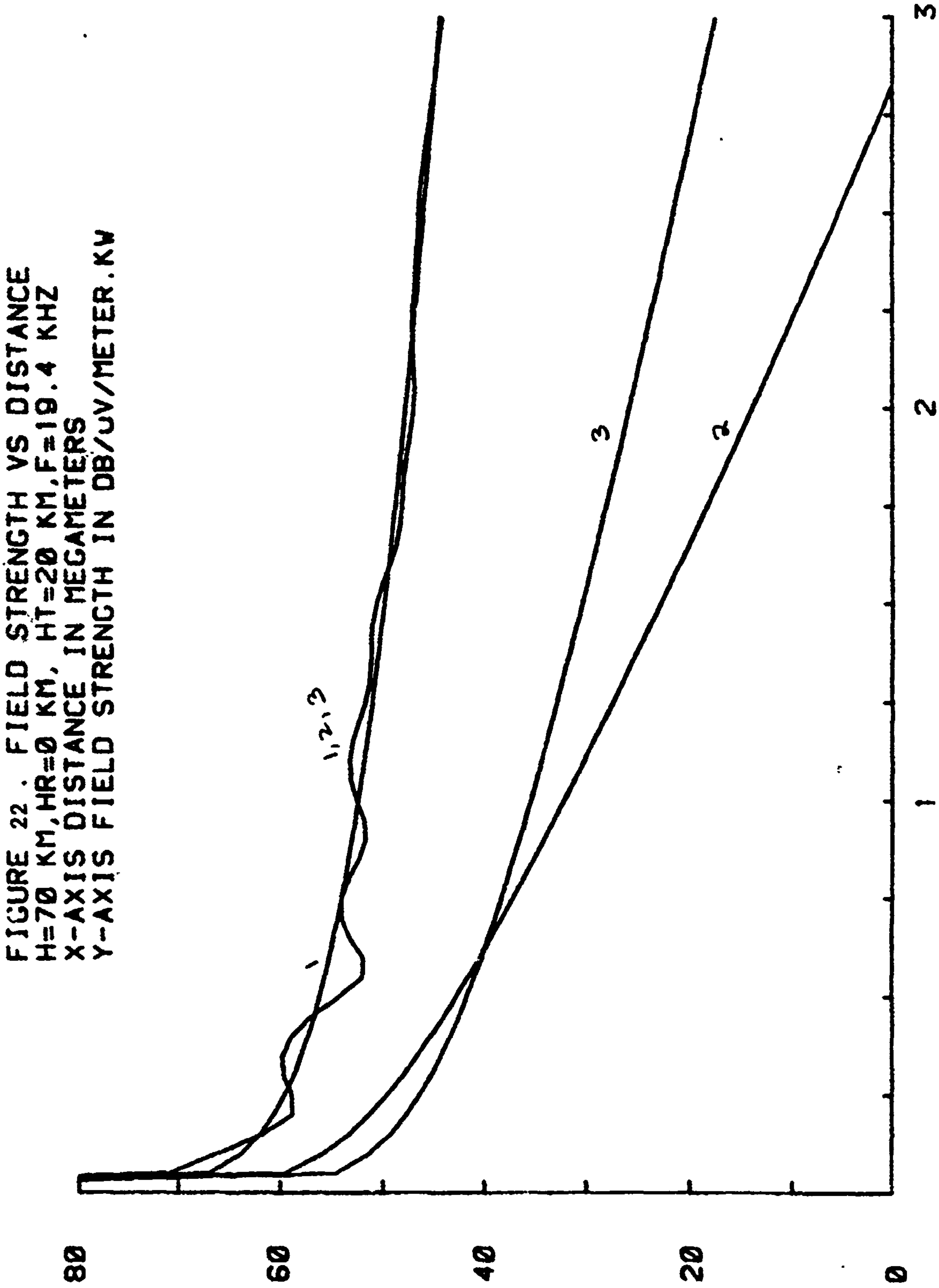

FIGURE 22 . FIELD STRENGTH VS DISTANCE
H=70 KM,HR=0 KM, HT=20 KM,F=19.4 KHZ
X-AXIS DISTANCE IN MEGAMETERS
Y-AXIS FIELD STRENGTH IN DB/UV/METER.KW

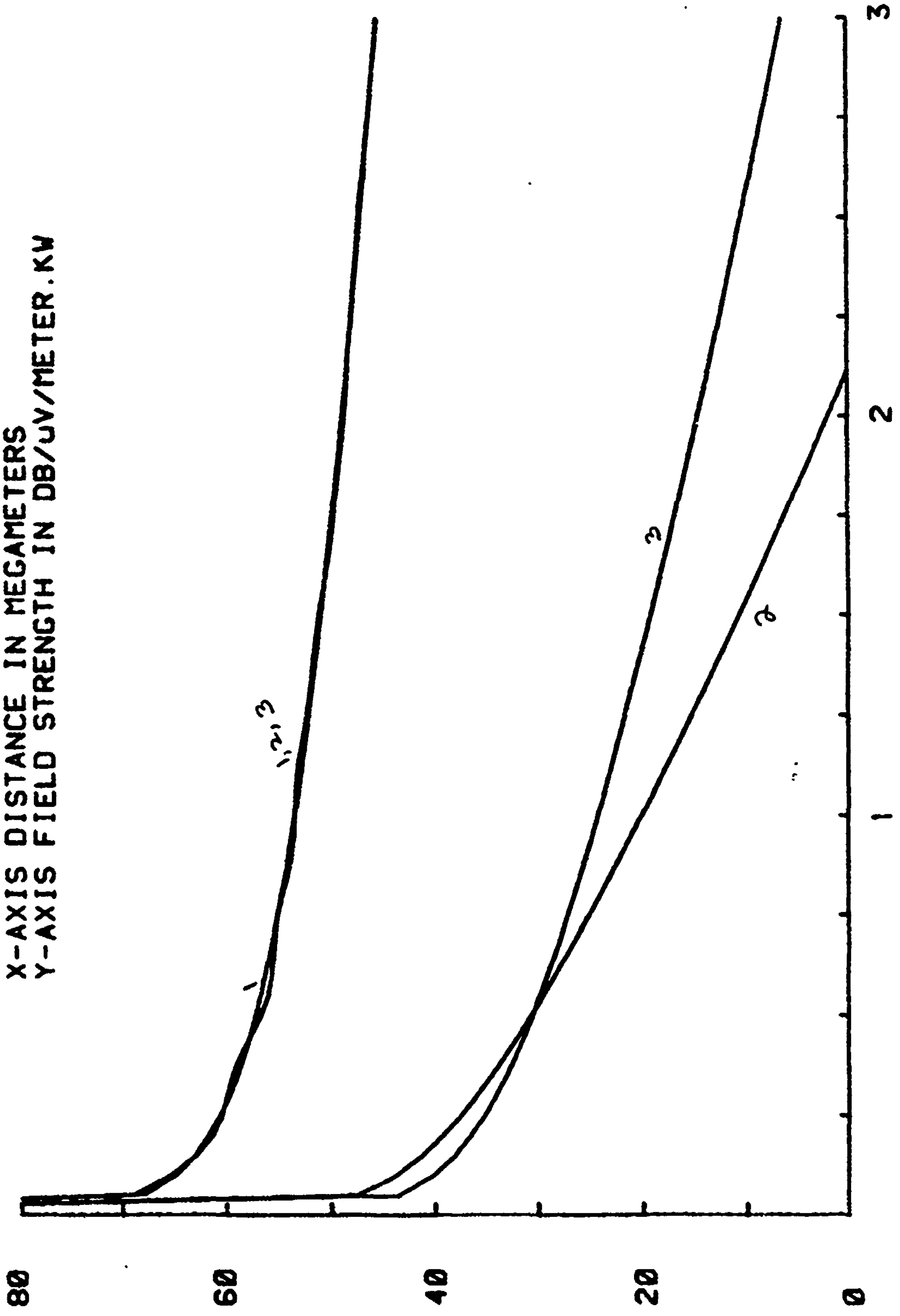

FIGURE 23. FIELD STRENGTH VS DISTANCE
H=70 KM,HR=0 KM, HT=30 KM,F=19.4 KHZ
X-AXIS DISTANCE IN MEGAMETERS
Y-AXIS FIELD STRENGTH IN DB/uV/METER.KW

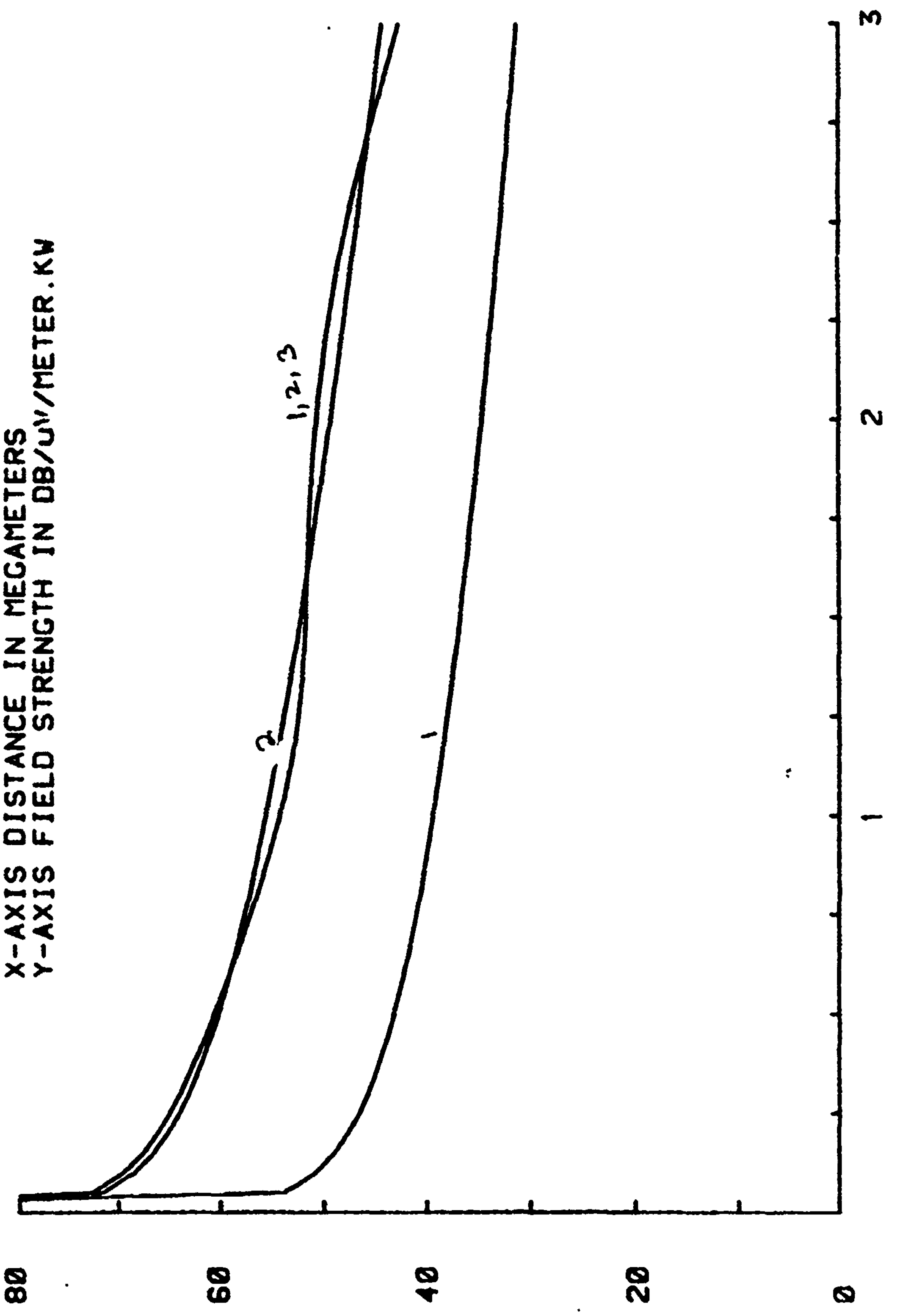

FIGURE 24 . FIELD STRENGTH VS DISTANCE
H=90 KM,HR=0 KM, HT=10 KM,F=19.4 KHZ
X-AXIS DISTANCE IN MEGAMETERS
Y-AXIS FIELD STRENGTH IN DB/UV/METER.KW

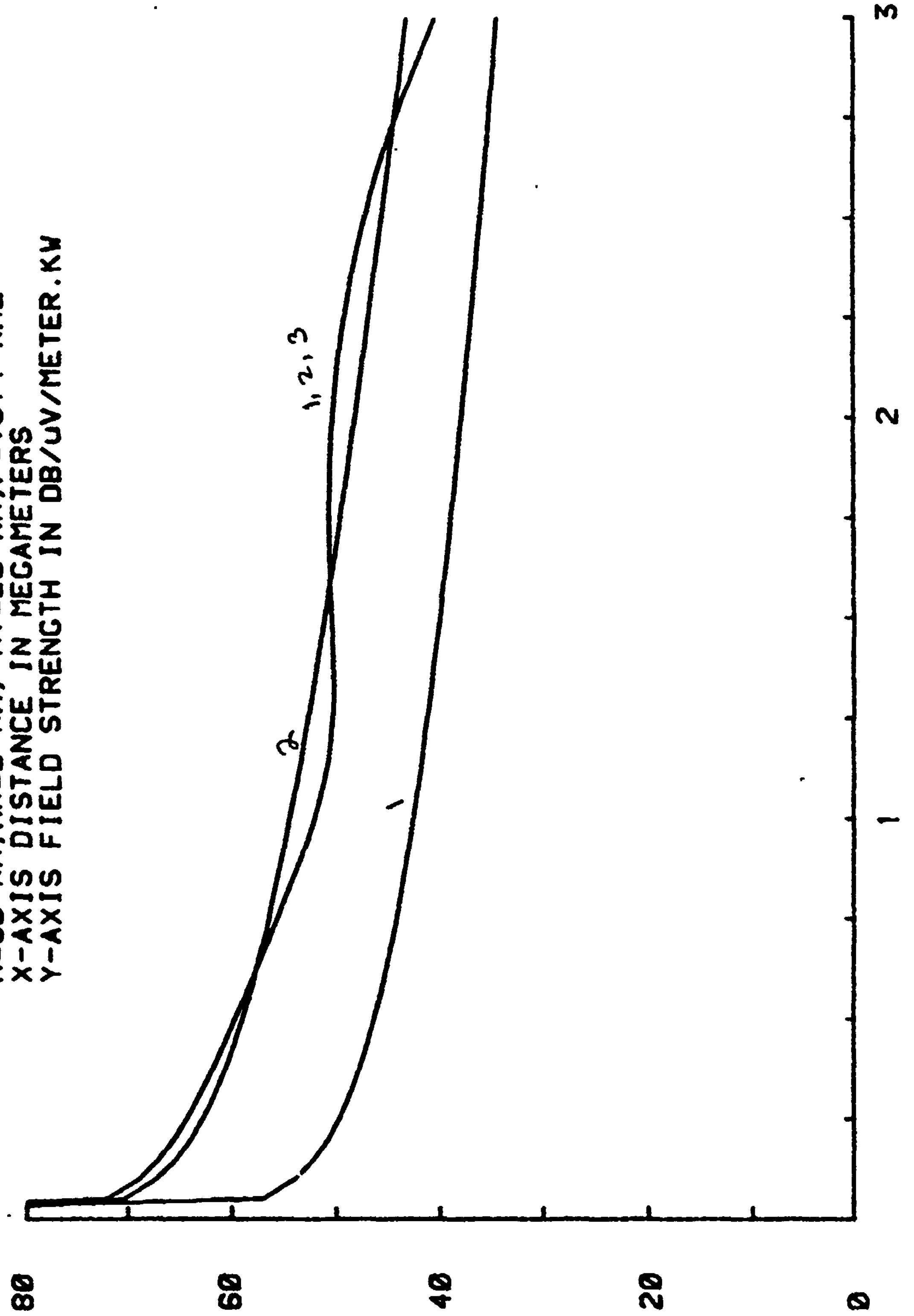

FIGURE 25. FIELD STRENGTH VS DISTANCE
H=90 KM,HR=0 KM, HT=20 KM,F=19.4 KHZ
X-AXIS DISTANCE IN MEGAMETERS
Y-AXIS FIELD STRENGTH IN DB/uV/METER.KW

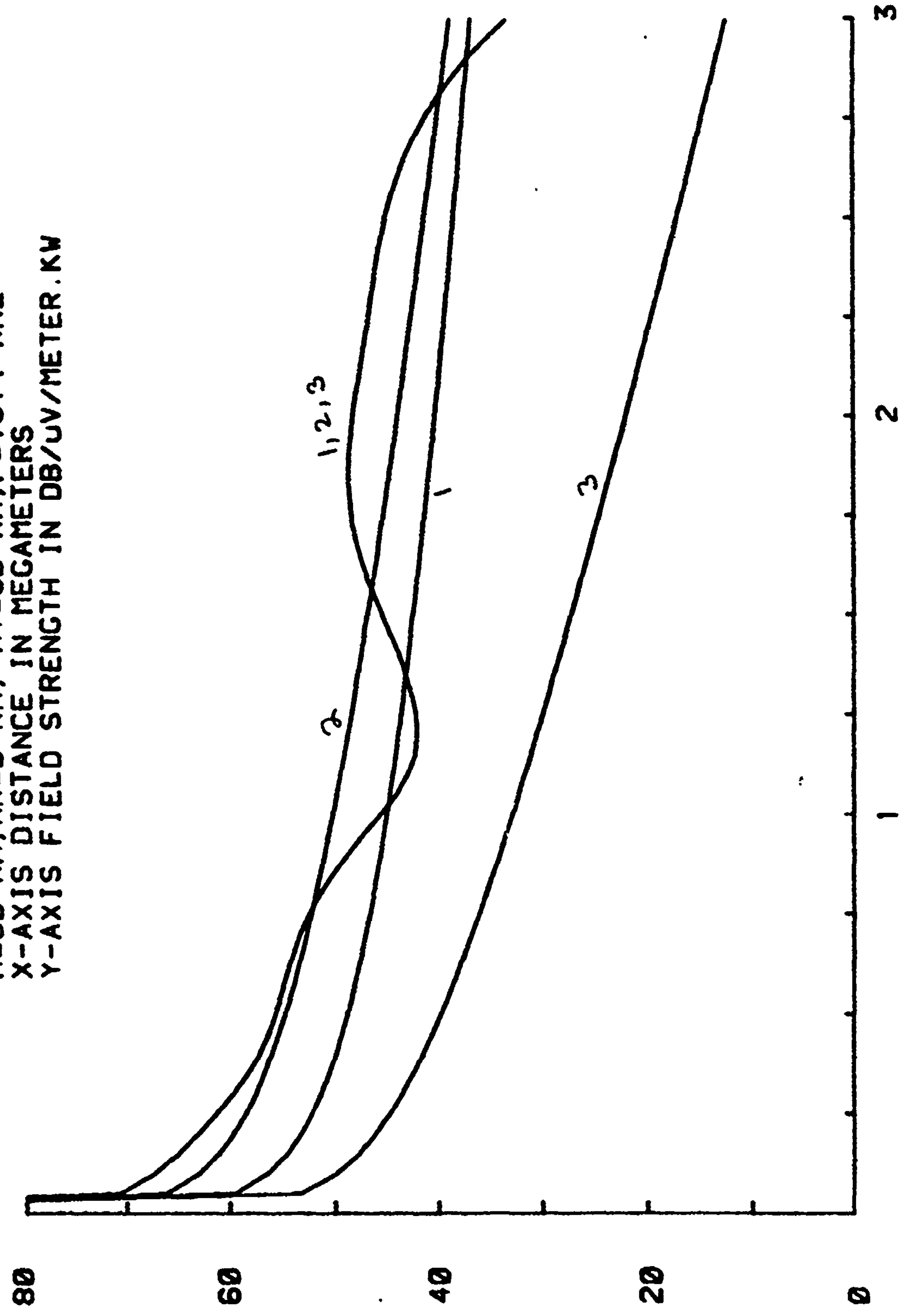

FIGURE 26. FIELD STRENGTH VS DISTANCE
H=90 KM,HR=0 KM, HT=30 KM,F=19.4 KHZ
X-AXIS DISTANCE IN MEGAMETERS
Y-AXIS FIELD STRENGTH IN DB/UV/METER.KW

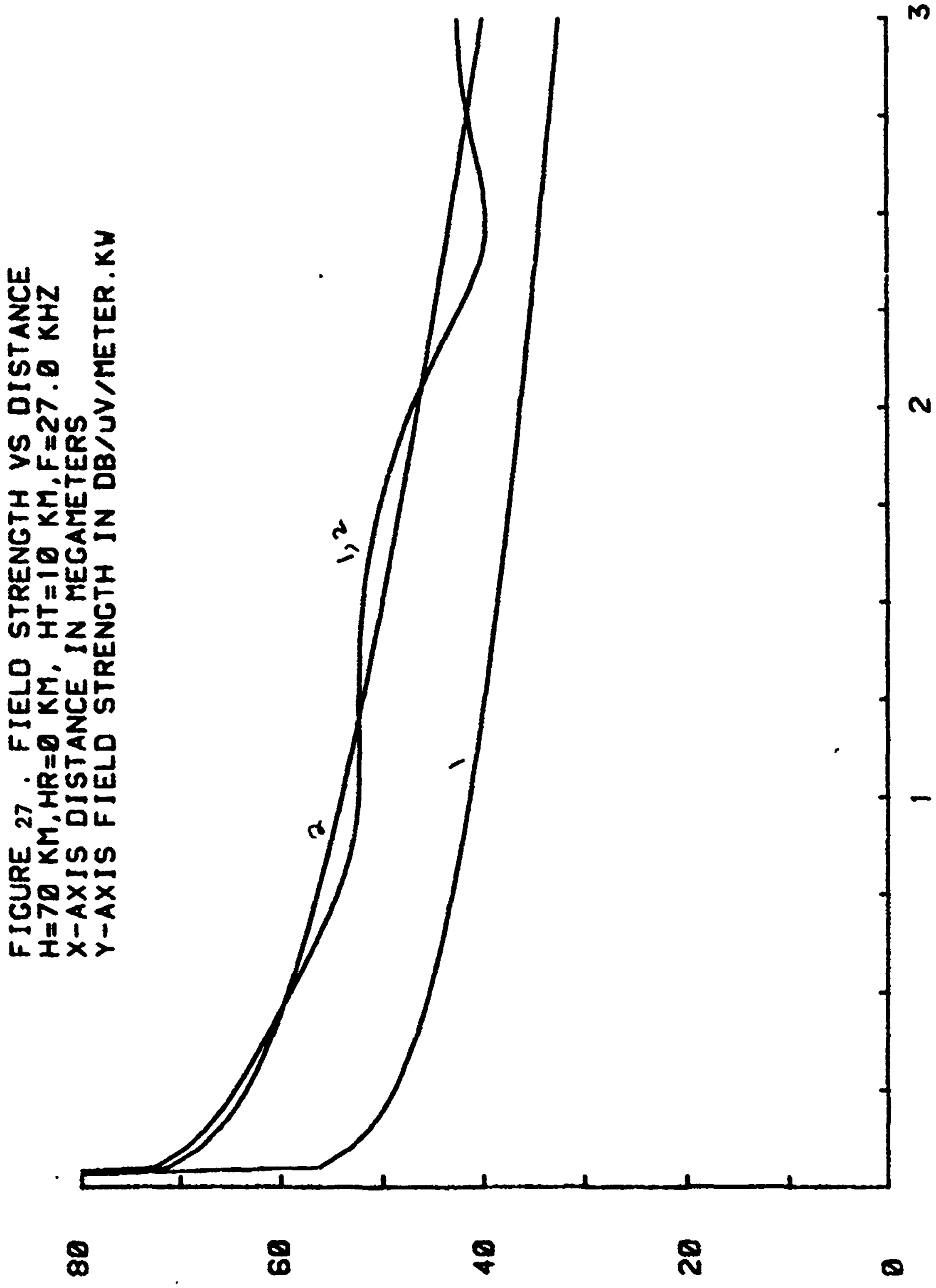

FIGURE 27 . FIELD STRENGTH VS DISTANCE
H=70 KM,HR=0 KM, HT=10 KM,F=27.0 KHZ
X-AXIS DISTANCE IN MEGAMETERS
Y-AXIS FIELD STRENGTH IN DB/uV/METER.KW

FIGURE 28 . FIELD STRENGTH VS DISTANCE
H=70 KM,HR=0 KM, HT=20 KM,F=27.0 KHZ
X-AXIS DISTANCE IN MEGAMETERS
Y-AXIS FIELD STRENGTH IN DB/uV/METER.KW

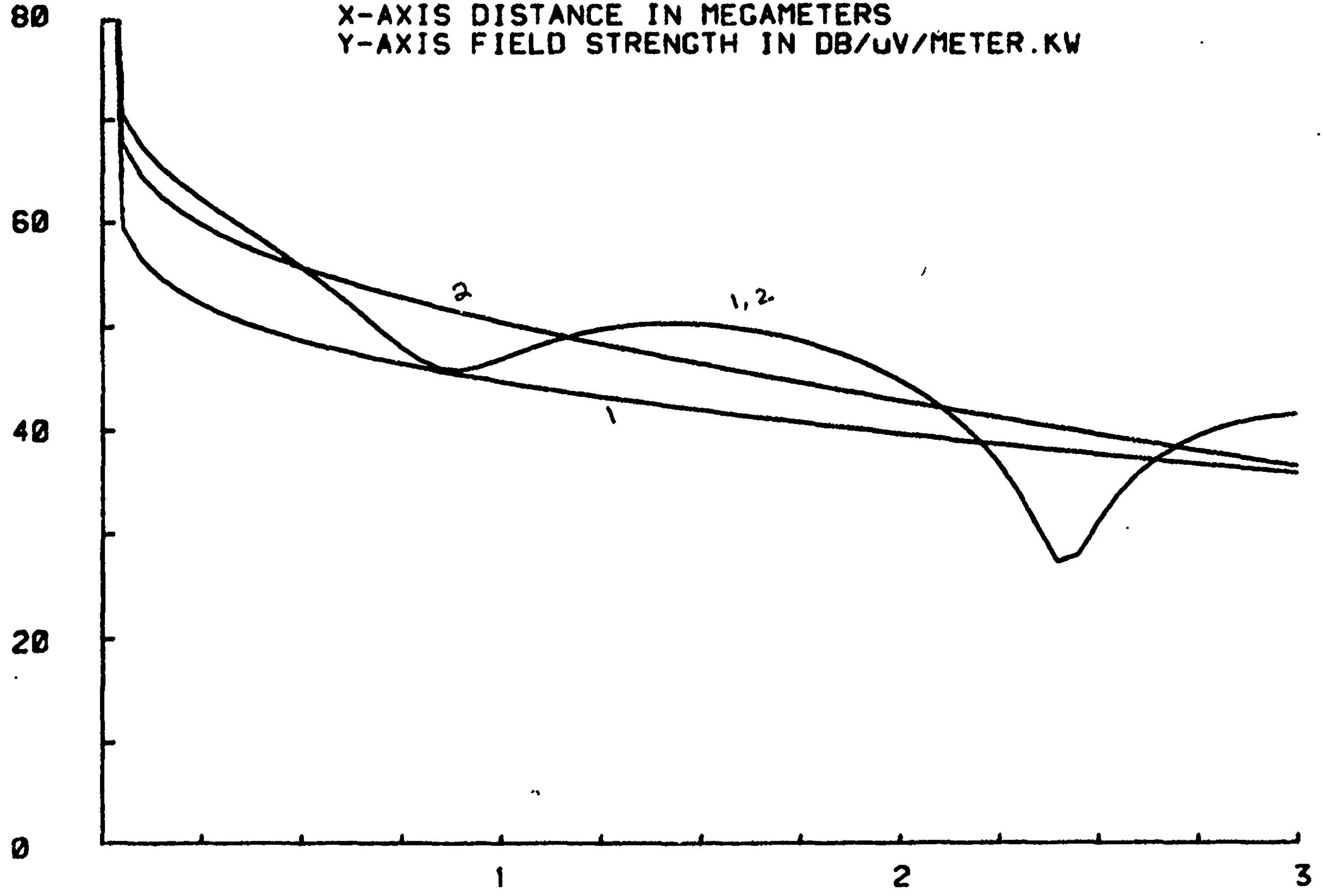

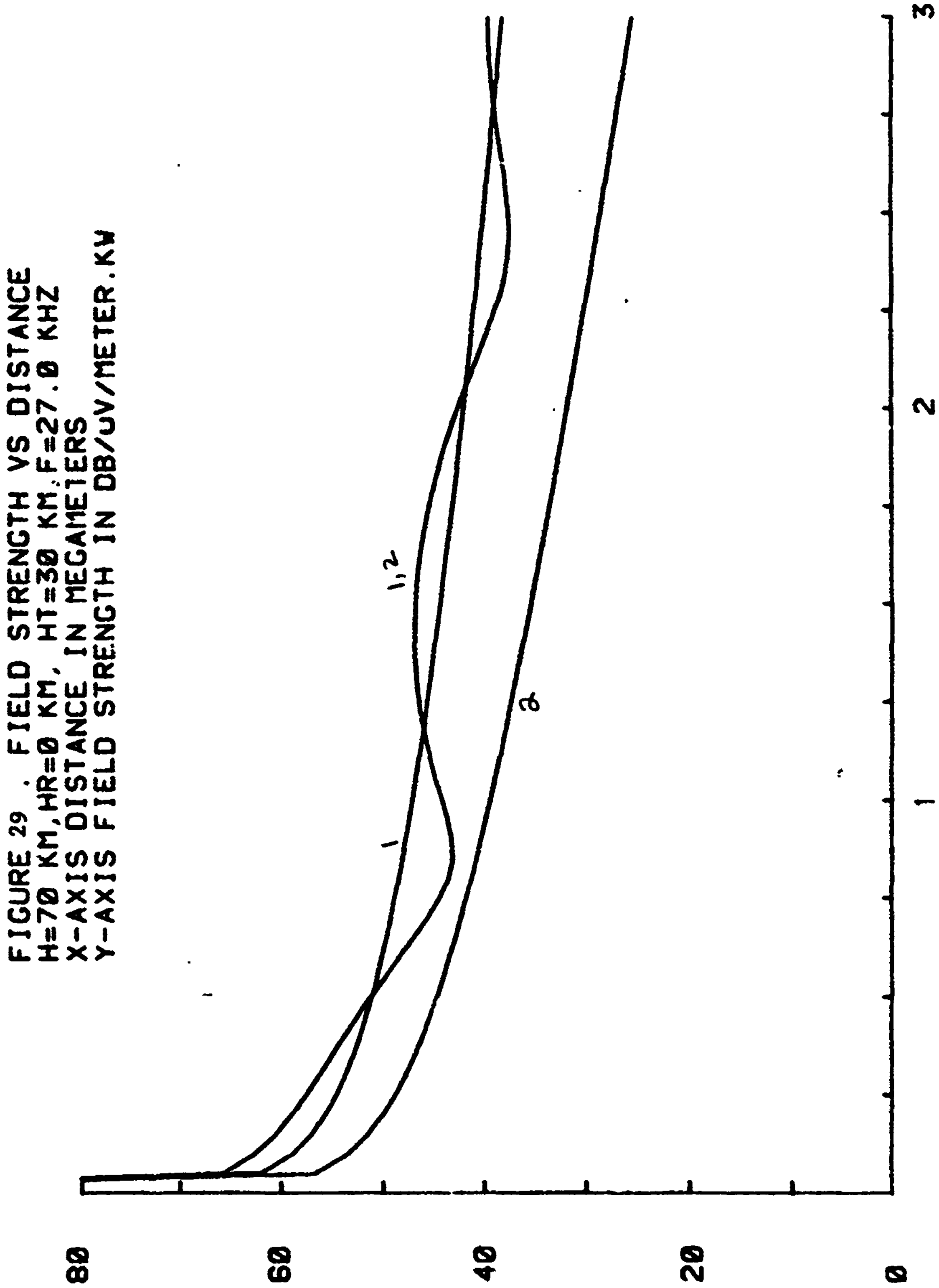

FIGURE 29 . FIELD STRENGTH VS DISTANCE
H=70 KM,HR=0 KM, HT=30 KM,F=27.0 KHZ
X-AXIS DISTANCE IN MEGAMETERS
Y-AXIS FIELD STRENGTH IN DB/UV/METER.KW

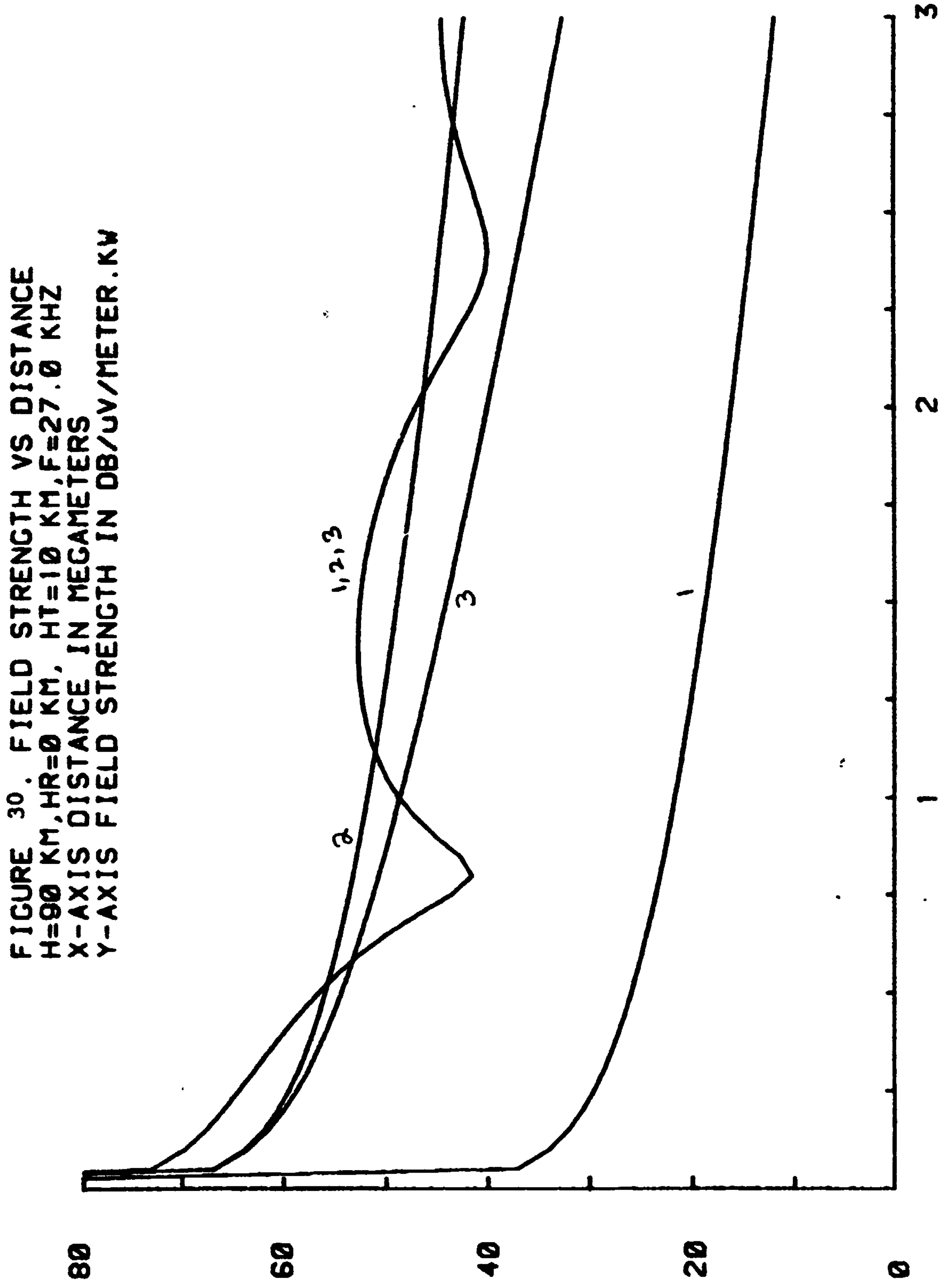

FIGURE 30. FIELD STRENGTH VS DISTANCE
H=90 KM,HR=0 KM, HT=10 KM,F=27.0 KHZ
X-AXIS DISTANCE IN MEGAMETERS
Y-AXIS FIELD STRENGTH IN DB/UV/METER.KW

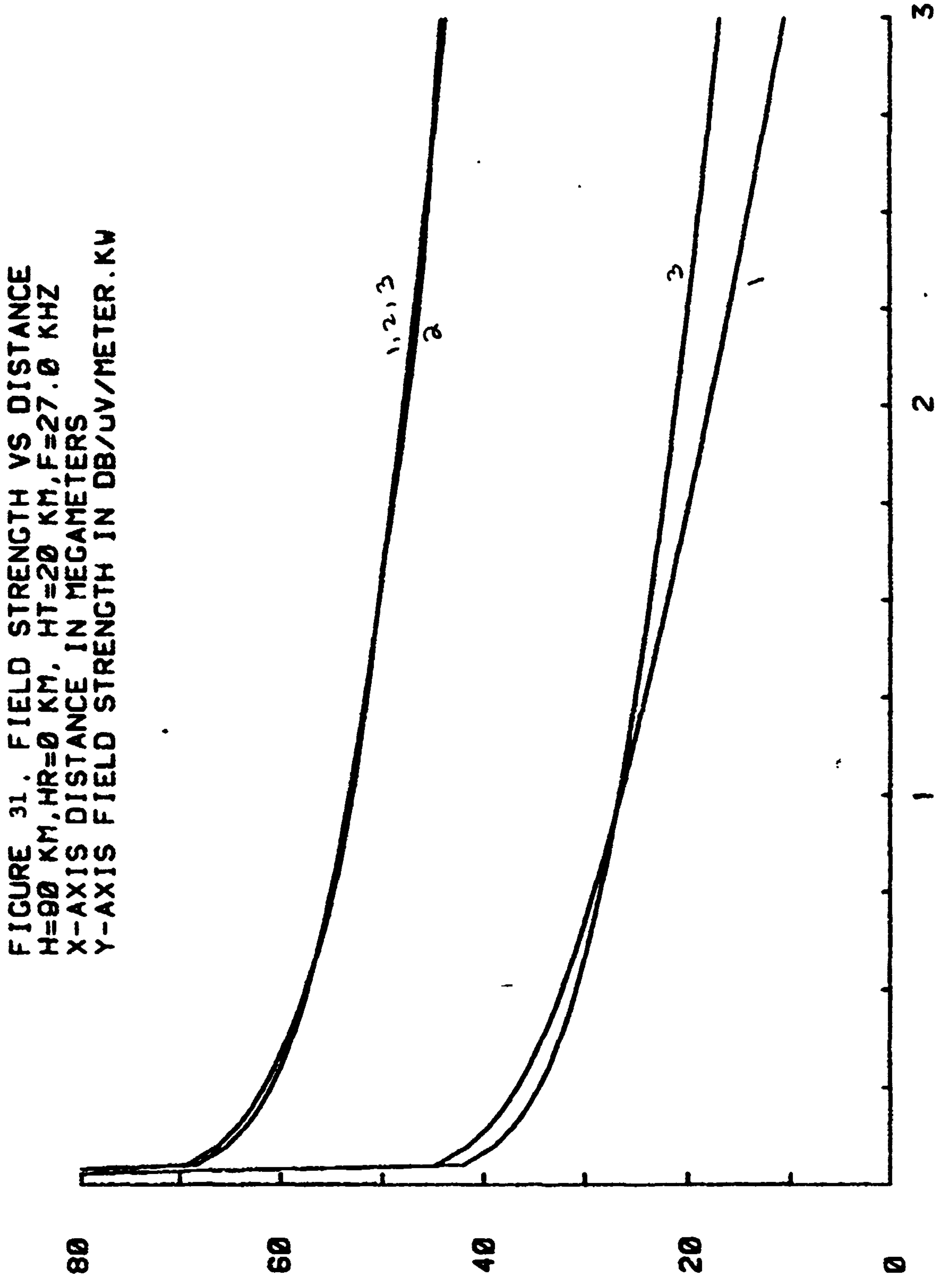

FIGURE 31. FIELD STRENGTH VS DISTANCE
H=90 KM,HR=0 KM, HT=20 KM,F=27.0 KHZ
X-AXIS DISTANCE IN MEGAMETERS
Y-AXIS FIELD STRENGTH IN DB/UV/METER.KW

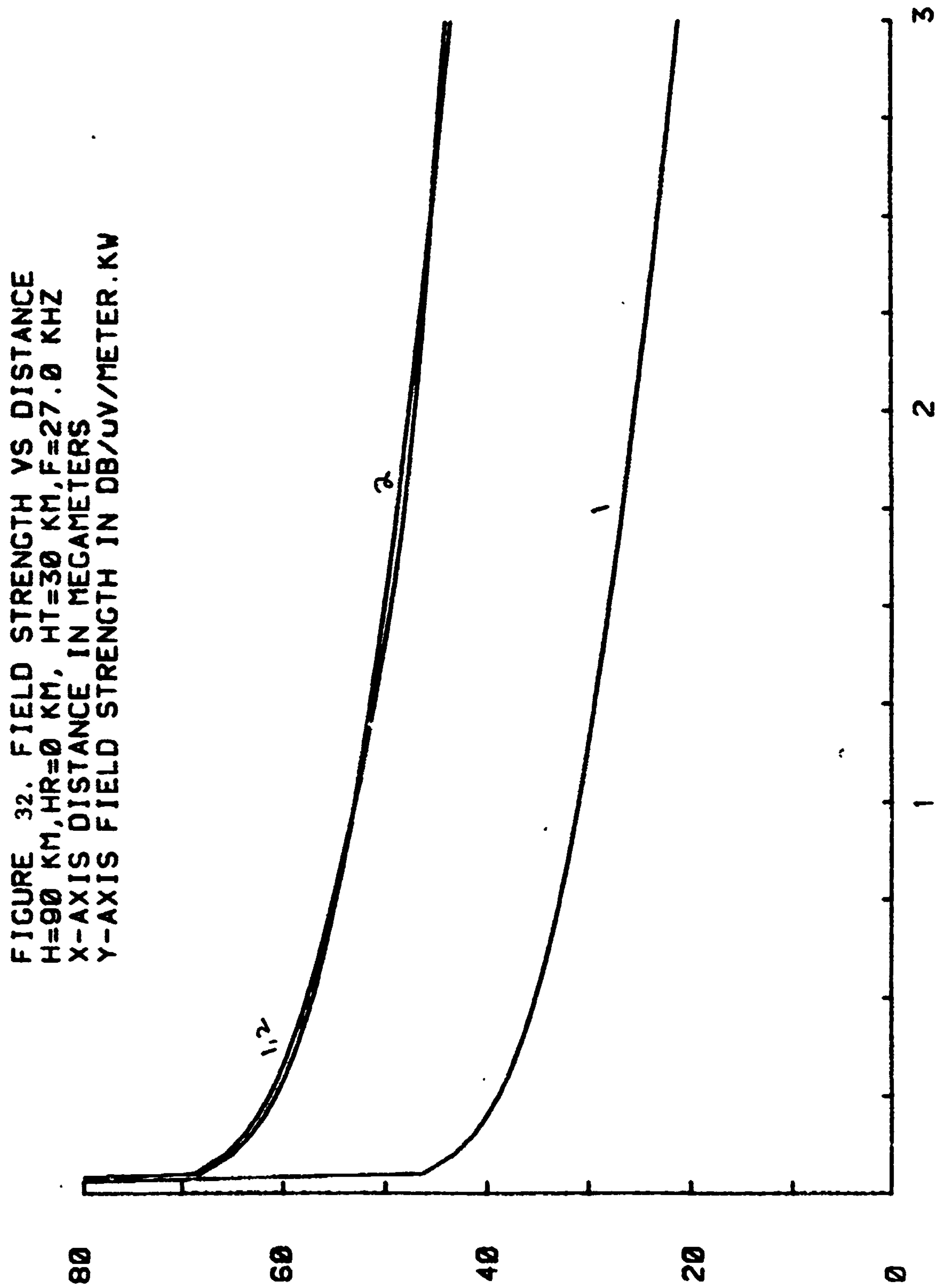

FIGURE 32. FIELD STRENGTH VS DISTANCE
H=90 KM,HR=0 KM, HT=30 KM,F=27.0 KHZ
X-AXIS DISTANCE IN MEGAMETERS
Y-AXIS FIELD STRENGTH IN DB/UV/METER.KW

INFLUENCE OF GEOMAGNETIC FIELD ON MODESUM AND INDIVIDUAL MODE FIELD STRENGTHS

In all the previous calculations, it has been tacitly assumed that the ionosphere is isotropic and is characterized by an exponential profile for electronic density and collisional frequency variations. This assumption neglects the presence of the earth's geomagnetic field. When the presence of this field is taken into consideration, the ionosphere becomes anisotropic and the characteristics of VLF radio propagation change, though in most cases these changes are very small. The presence of the geomagnetic field produces changes in the values of individual mode and modesum field strengths through the changes in the values of phase velocity, phase of the excitation factor and attenuation constant, especially when the propagation takes place along the East-to-West or West-to-East directions. It has been experimentally observed that the field strengths for the East-to-West propagation is weaker than for the West-to-East propagation, in clear violation of the principle of reciprocity for waveguide mode of propagation (9).

The plans for the balloon-to-balloon-borne communication experiment calls for one of the links to have East-to-West propagation (Kwajalein, the transmitting site to Guam, the receiving site). In order to make an estimate of the influence of the geomagnetic field on this communication link, some of the calculations - especially for the predominant mode (the first order mode) - have been repeated for an anisotropic ionosphere. The calculations are applicable for a field station with a dip angle of 7^{o}, which is the dip angle midway between Kwajalein-Guam link (data courtesy of the Geomagnetic Division, World Data Center A, Boulder, Colorado). The values of the various parameters for an anisotropic ionosphere are listed in Table V. Field strengths for the first order mode at 19.5 kHz as a function of distance for both the isotropic and anisotropic ionosphere hâve been presented in graphical forms in Figures 33 through 36. Results for the daytime condition with the transmitting and receiving antennas having the same elevations (either ground-based or 30 km) are shown in Figures 33 and 34. Figures 35 and 36 represent similar results for the nighttime condition. In all these figures, the top curve is for the isotropic ionosphere and the bottom curve for the anisotropic ionosphere. The corresponding numerical values of the field strengths and the differences of the field strengths are listed in tabular forms in Table VI through XVII. In all these analyses, it is found that the field strength differences occur with a maximum value of about 3 dB at a distance 3 Mm. Thus, the anisotropy of the ionosphere, though important, is not very significant.

TABLE V. PARAMETERS FOR ISOTROPIC AND ANISOTROPIC IONOSPHERE

f (KHz)	h (Km)	n	$\phi\Lambda 1$ (E→W)	$\phi\Lambda 1$ (N→S) ←	α (dB/Mm) (E→W)	α (dB/Mm) (N→S) ←	$\frac{v_{p1}}{c} - 1$ (E→W)	$\frac{v_{p1}}{c} - 1$ (N→S)
19.4	70	1	11.1	10	2.8	2.5	-0.11	-0.11
	90		20	18	2.75	2.45	-0.35	-0.35
27.0	70		20.1	19	3.75	3.4	-0.22	-0.22
	90		47	41	5.2	4.6	-0.52	-0.52

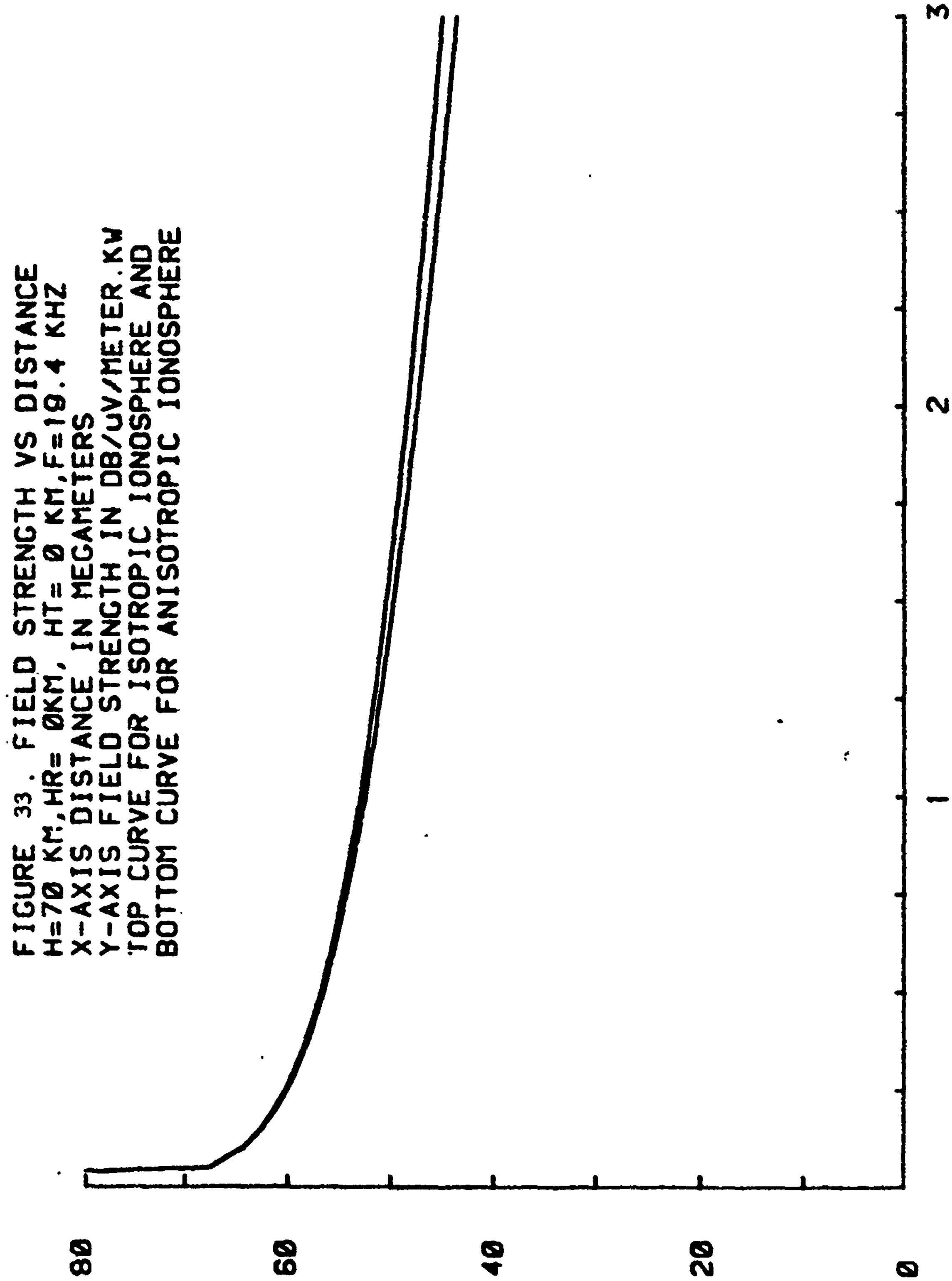

FIGURE 33 . FIELD STRENGTH VS DISTANCE
H=70 KM,HR= 0KM, HT= 0 KM,F=19.4 KHZ
X-AXIS DISTANCE IN MEGAMETERS
Y-AXIS FIELD STRENGTH IN DB/UV/METER.KW
TOP CURVE FOR ISOTROPIC IONOSPHERE AND
BOTTOM CURVE FOR ANISOTROPIC IONOSPHERE

RECEIVER ALTITUDE = Ø KM.   HGF = Ø.28 DB.

RANGE KM.	FIELD STRENGTH DB//UV.//KW
2ØØ	61.25
3ØØ	59.34
4ØØ	57.94
5ØØ	56.81
6ØØ	55.87
7ØØ	55.Ø4
8ØØ	54.31
9ØØ	53.65
1ØØØ	53.Ø4
11ØØ	52.47
12ØØ	51.94
13ØØ	51.44
14ØØ	5Ø.97
15ØØ	5Ø.52
16ØØ	5Ø.Ø9
17ØØ	49.68
18ØØ	49.28
19ØØ	48.9
2ØØØ	48.53
21ØØ	48.17
22ØØ	47.82
23ØØ	47.48
24ØØ	47.14
25ØØ	46.82
26ØØ	46.5
27ØØ	46.19
28ØØ	45.89
29ØØ	45.59
3ØØØ	45.3

TABLE VI. VALUES OF FIRST ORDER MODE FIELD STRENGTH VS DISTANCE FOR ISOTROPIC IONOSPHERE
($h_T = h_R = 0$, $h = 70$ km, $f = 19.4$ kHz)

RECEIVER ALTITUDE = 0 KM. HGF = 0.28 DB.

RANGE KM.	FIELD STRENGTH DB//UV.//KW
200	61.16
300	59.2
400	57.75
500	56.58
600	55.59
700	54.72
800	53.94
900	53.23
1000	52.57
1100	51.96
1200	51.38
1300	50.84
1400	50.32
1500	49.82
1600	49.34
1700	48.89
1800	48.44
1900	48.01
2000	47.59
2100	47.19
2200	46.79
2300	46.4
2400	46.02
2500	45.65
2600	45.29
2700	44.93
2800	44.58
2900	44.24
3000	43.9

TABLE VII. VALUES OF FIRST ORDER MODE FIELD STRENGTH VS DISTANCE FOR ANISOTROPIC IONOSPHERE ($h_T = h_R = 0$, $h = 70$ km , $f = 19.4$ kHz)

1	0.02	2	0.04	3	0.06	4	0.09
5	0.11	6	0.13	7	0.16	8	0.18
9	0.2	10	0.23	11	0.25	12	0.27
13	0.3	14	0.32	15	0.34	16	0.37
17	0.39	18	0.41	19	0.44	20	0.46
21	0.48	22	0.51	23	0.53	24	0.55
25	0.58	26	0.6	27	0.62	28	0.65
29	0.67	30	0.69	31	0.72	32	0.74
33	0.76	34	0.79	35	0.81	36	0.83
37	0.86	38	0.88	39	0.9	40	0.93
41	0.95	42	0.97	43	0.99	44	1.02
45	1.04	46	1.06	47	1.09	48	1.11
49	1.13	50	1.16	51	1.18	52	1.2
53	1.23	54	1.25	55	1.27	56	1.3
57	1.32	58	1.34	59	1.37	60	1.39
61	1.41	62	1.44	63	1.46	64	1.48
65	1.51	66	1.53	67	1.55	68	1.58
69	1.6	70	1.62	71	1.65	72	1.67
73	1.69	74	1.72	75	1.74	76	1.76
77	1.79	78	1.81	79	1.83	80	1.85
81	1.88	82	1.9	83	1.92	84	1.95
85	1.97	86	1.99	87	2.02	88	2.04
89	2.06	90	2.09	91	2.11	92	2.13
93	2.16	94	2.18	95	2.2	96	2.23
97	2.25	98	2.27	99	2.3	100	2.32
101	2.34	102	2.37	103	2.39	104	2.41
105	2.44	106	2.46	107	2.48	108	2.51
109	2.53	110	2.55	111	2.58	112	2.6
113	2.62	114	2.65	115	2.67	116	2.69
117	2.72	118	2.74	119	2.76	120	2.78

FIELD STRENGTH DIFFERENCE (DB.uV/METER.KW) VS DISTANCE (NUMBER X 25 KM)
F=19.4 KHZ, H=70 KM, HT=HR=0 KM, n=1

TABLE VIII.

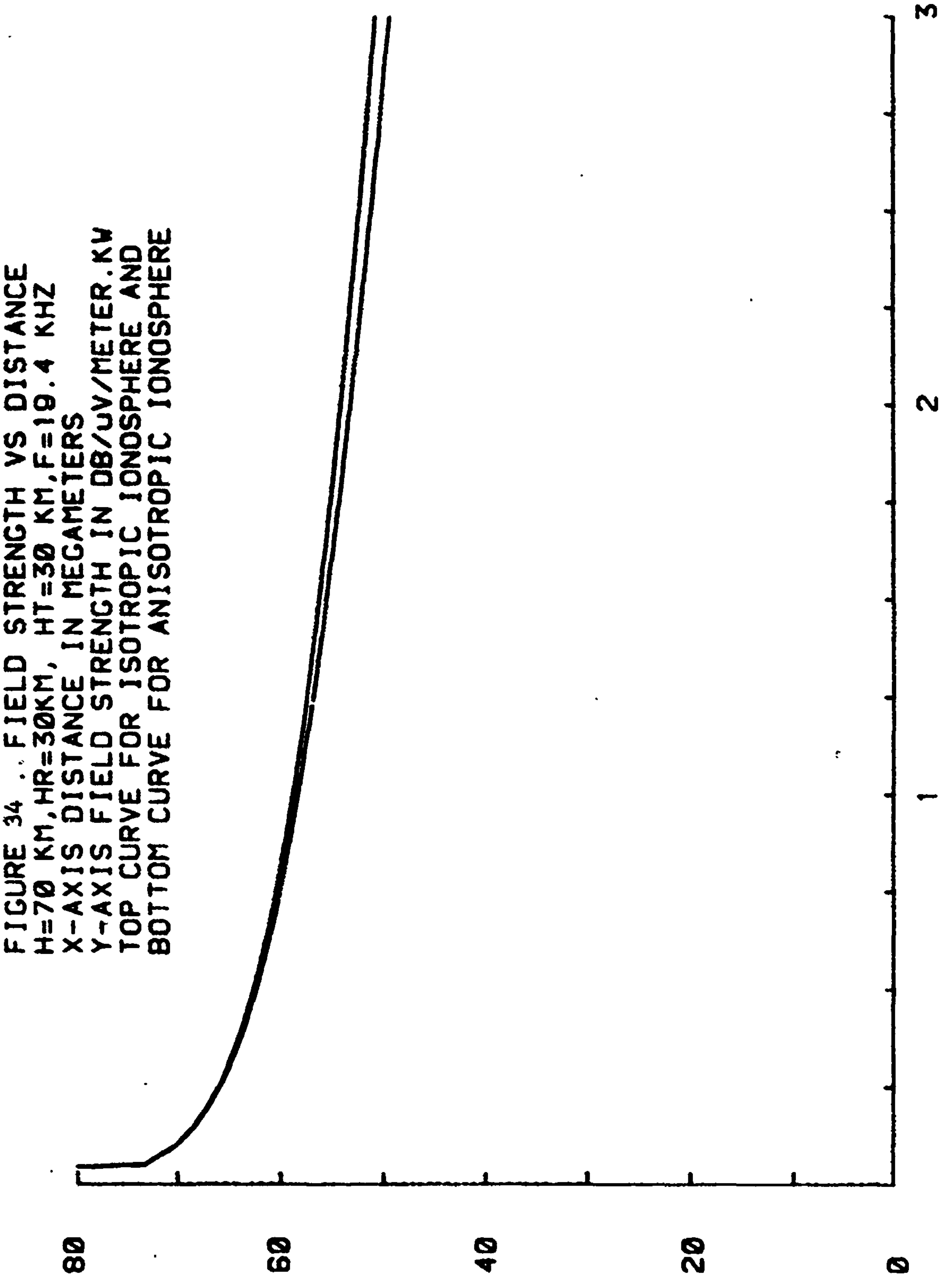

FIGURE 34 .. FIELD STRENGTH VS DISTANCE
H=70 KM,HR=30KM, HT=30 KM,F=19.4 KHZ
X-AXIS DISTANCE IN MEGAMETERS
Y-AXIS FIELD STRENGTH IN DB/uV/METER.KW
TOP CURVE FOR ISOTROPIC IONOSPHERE AND
BOTTOM CURVE FOR ANISOTROPIC IONOSPHERE

RECEIVER ALTITUDE = 30 KM.   HGF = 6.03 DB.

RANGE KM.	FIELD STRENGTH DB//UV.//KW
200	67
300	65.09
400	63.69
500	62.56
600	61.62
700	60.79
800	60.06
900	59.4
1000	58.79
1100	58.22
1200	57.69
1300	57.19
1400	56.72
1500	56.27
1600	55.84
1700	55.43
1800	55.03
1900	54.65
2000	54.28
2100	53.92
2200	53.57
2300	53.23
2400	52.89
2500	52.57
2600	52.25
2700	51.94
2800	51.64
2900	51.34
3000	51.05

TABLE IX. VALUES OF FIRST ORDER MODE FIELD STRENGTH VS DISANCE FOR ISOTROPIC IONOSPHERE ($h_T = h_R = 30$ km, $h = 70$ km, $f = 19.4$ kHz)

RECEIVER ALTITUDE = 30 KM.   HGF = 6.03 DB.

RANGE KM.	FIELD STRENGTH DB//UV.//KW
200	66.91
300	64.95
400	63.5
500	62.33
600	61.34
700	60.47
800	59.69
900	58.98
1000	58.32
1100	57.71
1200	57.13
1300	56.59
1400	56.07
1500	55.57
1600	55.09
1700	54.64
1800	54.19
1900	53.76
2000	53.34
2100	52.94
2200	52.54
2300	52.15
2400	51.77
2500	51.4
2600	51.04
2700	50.68
2800	50.33
2900	49.99
3000	49.65

TABLE X. VALUES OF FIRST ORDER MODE FIELD STRENGTH VS DISTANCE FOR ANISOTROPIC IONOSPHERE ($h_T = h_R = 30$ km, $h = 70$ km, $f = 19.4$ kHz)

1	0.02	2	0.04	3	0.06	4	0.09
5	0.11	6	0.13	7	0.16	8	0.18
9	0.2	10	0.23	11	0.25	12	0.27
13	0.3	14	0.32	15	0.34	16	0.37
17	0.39	18	0.41	19	0.44	20	0.46
21	0.48	22	0.51	23	0.53	24	0.55
25	0.58	26	0.6	27	0.62	28	0.65
29	0.67	30	0.69	31	0.72	32	0.74
33	0.76	34	0.79	35	0.81	36	0.83
37	0.86	38	0.88	39	0.9	40	0.92
41	0.95	42	0.97	43	0.99	44	1.02
45	1.04	46	1.06	47	1.09	48	1.11
49	1.13	50	1.16	51	1.18	52	1.2
53	1.23	54	1.25	55	1.27	56	1.3
57	1.32	58	1.34	59	1.37	60	1.39
61	1.41	62	1.44	63	1.46	64	1.48
65	1.51	66	1.53	67	1.55	68	1.58
69	1.6	70	1.62	71	1.65	72	1.67
73	1.69	74	1.72	75	1.74	76	1.76
77	1.79	78	1.81	79	1.83	80	1.85
81	1.88	82	1.9	83	1.92	84	1.95
85	1.97	86	1.99	87	2.02	88	2.04
89	2.06	90	2.09	91	2.11	92	2.13
93	2.16	94	2.18	95	2.2	96	2.23
97	2.25	98	2.27	99	2.3	100	2.32
101	2.34	102	2.37	103	2.39	104	2.41
105	2.44	106	2.46	107	2.48	108	2.51
109	2.53	110	2.55	111	2.58	112	2.6
113	2.62	114	2.65	115	2.67	116	2.69
117	2.72	118	2.74	119	2.76	120	2.78

TABLE XI. VALUES OF THE DIFFERENCE BETWEEN FIRST ORDER MODE FIELD STRENGTH VS DISTANCE FOR ISOTROPIC AND ANISOTROPIC IONOSPHERE .
($h_T = h_R = 30$ km, $h = 70$ km, $f = 19.4$ kHz)

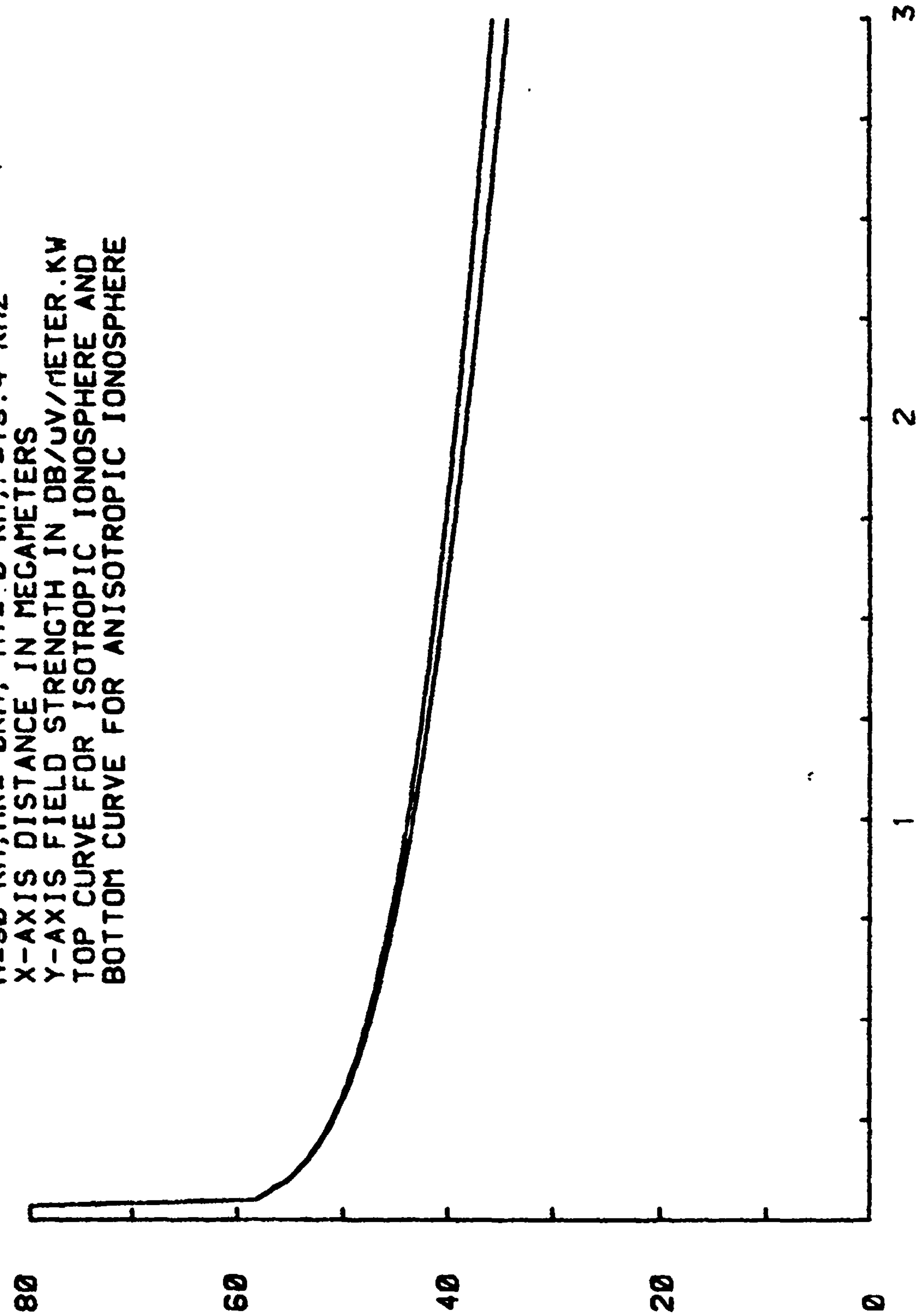

FIGURE 35 . FIELD STRENGTH VS DISTANCE
H=90 KM,HR= 0KM, HT= 0 KM,F=19.4 KHZ
X-AXIS DISTANCE IN MEGAMETERS
Y-AXIS FIELD STRENGTH IN DB/uV/METER.KW
TOP CURVE FOR ISOTROPIC IONOSPHERE AND
BOTTOM CURVE FOR ANISOTROPIC IONOSPHERE

RECEIVER ALTITUDE = 0 KM.   HGF = -8.84 DB.

RANGE KM.	FIELD STRENGTH DB//UV.//KW
200	50.92
300	49
400	47.59
500	46.46
600	45.51
700	44.68
800	43.94
900	43.27
1000	42.65
1100	42.08
1200	41.54
1300	41.04
1400	40.56
1500	40.1
1600	39.67
1700	39.25
1800	38.84
1900	38.45
2000	38.08
2100	37.71
2200	37.35
2300	37.01
2400	36.67
2500	36.34
2600	36.01
2700	35.7
2800	35.39
2900	35.08
3000	34.78

TABLE XII. VALUES OF FIRST ORDER MODE FIELD STRENGTH VS DISTANCE FOR ISOTROPIC IONOSPHERE ($h_T = h_R = 0$, $h = 90$ km, $f = 19.4$ kHz)

RECEIVER ALTITUDE = 0 KM.   HGF = -8.84 DB.

RANGE KM.	FIELD STRENGTH DB//UV.//KW
200	50.82
300	48.85
400	47.39
500	46.22
600	45.22
700	44.34
800	43.55
900	42.83
1000	42.17
1100	41.55
1200	40.96
1300	40.41
1400	39.88
1500	39.37
1600	38.89
1700	38.42
1800	37.97
1900	37.53
2000	37.1
2100	36.69
2200	36.28
2300	35.89
2400	35.5
2500	35.12
2600	34.75
2700	34.38
2800	34.03
2900	33.67
3000	33.33

TABLE XIII. VALUES OF FIRST ORDER MODE FIELD STRENGTH VS DISTANCE FOR ANISOTROPIC IONOSPHERE ($h_T = h_R = 0$, $h = 90$ km, $f = 19.4$ kHz)

1	0.02	2	0.04	3	0.07	4	0.09
5	0.12	6	0.14	7	0.17	8	0.19
9	0.21	10	0.24	11	0.26	12	0.29
13	0.31	14	0.34	15	0.36	16	0.38
17	0.41	18	0.43	19	0.46	20	0.48
21	0.51	22	0.53	23	0.55	24	0.58
25	0.6	26	0.63	27	0.65	28	0.68
29	0.7	30	0.72	31	0.75	32	0.77
33	0.8	34	0.82	35	0.85	36	0.87
37	0.89	38	0.92	39	0.94	40	0.97
41	0.99	42	1.02	43	1.04	44	1.06
45	1.09	46	1.11	47	1.14	48	1.16
49	1.19	50	1.21	51	1.23	52	1.26
53	1.28	54	1.31	55	1.33	56	1.36
57	1.38	58	1.4	59	1.43	60	1.45
61	1.48	62	1.5	63	1.53	64	1.55
65	1.57	66	1.6	67	1.62	68	1.65
69	1.67	70	1.7	71	1.72	72	1.74
73	1.77	74	1.79	75	1.82	76	1.84
77	1.87	78	1.89	79	1.91	80	1.94
81	1.96	82	1.99	83	2.01	84	2.04
85	2.06	86	2.08	87	2.11	88	2.13
89	2.16	90	2.18	91	2.21	92	2.23
93	2.25	94	2.28	95	2.3	96	2.33
97	2.35	98	2.38	99	2.4	100	2.42
101	2.45	102	2.47	103	2.5	104	2.52
105	2.55	106	2.57	107	2.6	108	2.62
109	2.64	110	2.67	111	2.69	112	2.72
113	2.74	114	2.77	115	2.79	116	2.81
117	2.84	118	2.86	119	2.89	120	2.91

FIELD STRENGTH DIFFERENCE (DB.uV/METER.KW) VS DISTANCE (NUMBER.X 25 KM)
F=19.4 KHZ, HR=0 KM, HT=00 KM, H=90 KM, n=1

TABLE XIV.

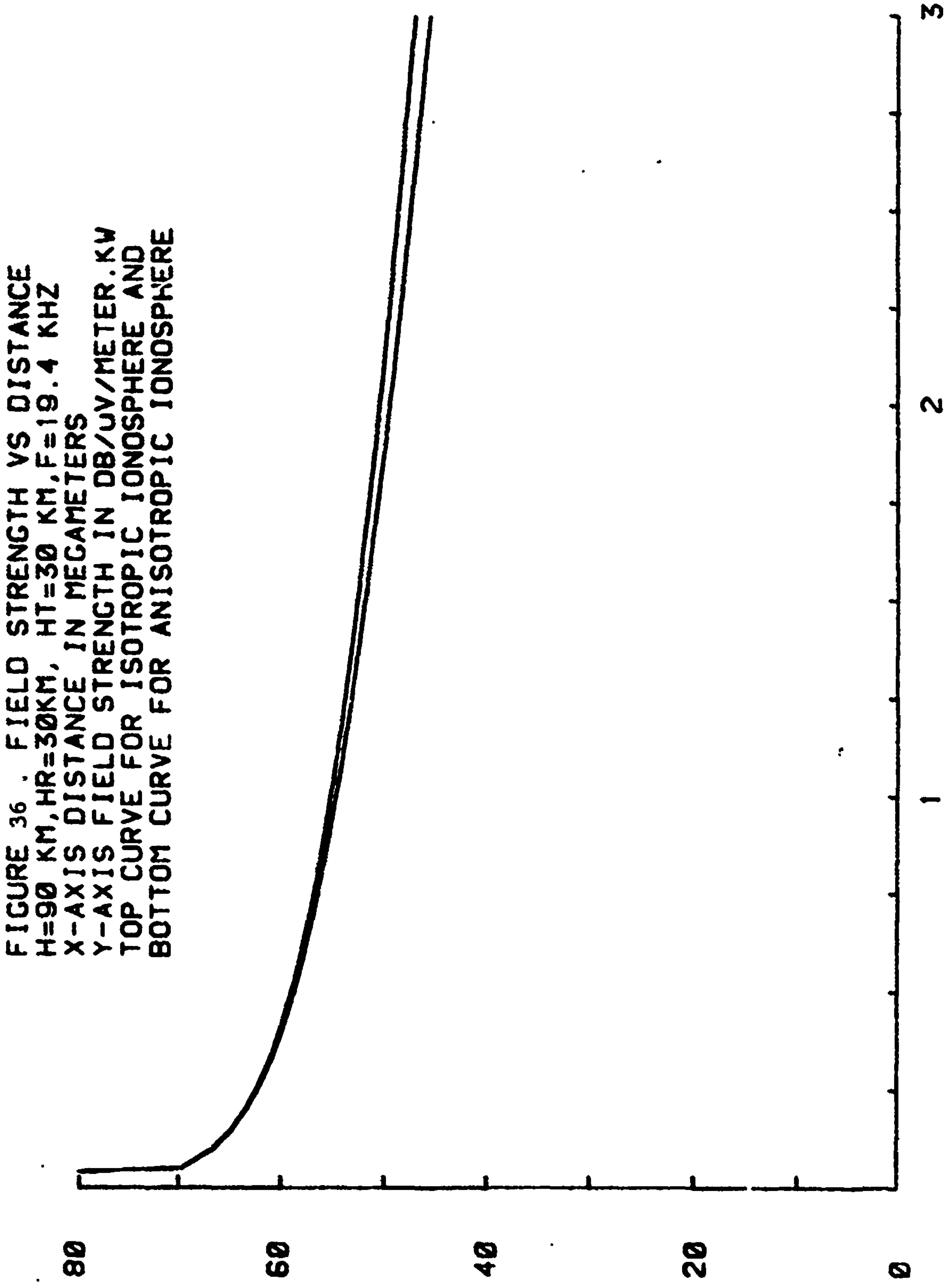

FIGURE 36 . FIELD STRENGTH VS DISTANCE
H=90 KM,HR=30KM, HT=30 KM,F=19.4 KHZ
X-AXIS DISTANCE IN MEGAMETERS
Y-AXIS FIELD STRENGTH IN DB/UV/METER.KW
TOP CURVE FOR ISOTROPIC IONOSPHERE AND
BOTTOM CURVE FOR ANISOTROPIC IONOSPHERE

RECEIVER ALTITUDE = 30 KM.   HGF = 2.47 DB.

RANGE KM.	FIELD STRENGTH DB//UV.//KW
200	62.23
300	60.31
400	58.9
500	57.77
600	56.82
700	55.99
800	55.25
900	54.58
1000	53.96
1100	53.39
1200	52.85
1300	52.35
1400	51.87
1500	51.41
1600	50.98
1700	50.56
1800	50.15
1900	49.76
2000	49.39
2100	49.02
2200	48.66
2300	48.32
2400	47.98
2500	47.65
2600	47.32
2700	47.01
2800	46.7
2900	46.39
3000	46.09

TABLE XV. VALUES OF THE FIRST ORDER MODE FIELD STRENGTH VS DISTANCE FOR ISOTROPIC IONOSPHERE ($h_T = h_R = 30$ km, $h = 90$ km, $f = 19.4$ kHz)

RECEIVER ALTITUDE = 30 KM.   HGF = 2.47 DB.

RANGE KM.	FIELD STRENGTH DB//UV.//KW
200	62.13
300	60.16
400	58.7
500	57.53
600	56.53
700	55.65
800	54.86
900	54.14
1000	53.48
1100	52.86
1200	52.27
1300	51.72
1400	51.19
1500	50.68
1600	50.2
1700	49.73
1800	49.28
1900	48.84
2000	48.41
2100	48
2200	47.59
2300	47.2
2400	46.81
2500	46.43
2600	46.06
2700	45.69
2800	45.34
2900	44.98
3000	44.64

TABLE XVI. VALUES OF THE FIRST ORDER MODE FIELD STRENGTH VS DISTANCE FOR ANISOTROPIC IONOSPHERE ($h_T = h_R = 30$ km, $h = 90$ km, $f = 19.4$ kHz)

1	0.02	2	0.04	3	0.07	4	0.09
5	0.12	6	0.14	7	0.17	8	0.19
9	0.21	10	0.24	11	0.26	12	0.29
13	0.31	14	0.34	15	0.36	16	0.38
17	0.41	18	0.43	19	0.46	20	0.48
21	0.51	22	0.53	23	0.55	24	0.58
25	0.6	26	0.63	27	0.65	28	0.68
29	0.7	30	0.72	31	0.75	32	0.77
33	0.8	34	0.82	35	0.85	36	0.87
37	0.89	38	0.92	39	0.94	40	0.97
41	0.99	42	1.02	43	1.04	44	1.06
45	1.09	46	1.11	47	1.14	48	1.16
49	1.19	50	1.21	51	1.23	52	1.26
53	1.28	54	1.31	55	1.33	56	1.36
57	1.38	58	1.4	59	1.43	60	1.45
61	1.48	62	1.5	63	1.53	64	1.55
65	1.57	66	1.6	67	1.62	68	1.65
69	1.67	70	1.7	71	1.72	72	1.74
73	1.77	74	1.79	75	1.82	76	1.84
77	1.87	78	1.89	79	1.91	80	1.94
81	1.96	82	1.99	83	2.01	84	2.04
85	2.06	86	2.08	87	2.11	88	2.13
89	2.16	90	2.18	91	2.21	92	2.23
93	2.25	94	2.28	95	2.3	96	2.33
97	2.35	98	2.38	99	2.4	100	2.42
101	2.45	102	2.47	103	2.5	104	2.52
105	2.55	106	2.57	107	2.6	108	2.62
109	2.64	110	2.67	111	2.69	112	2.72
113	2.74	114	2.77	115	2.79	116	2.81
117	2.84	118	2.86	119	2.89	120	2.91

TABLE XVII. VALUES OF THE DIFFERENCE BETWEEN FIRST ORDER MODE FIELD STRENGTH VS DISTANCE FOR ISOTROPIC AND ANISOTROPIC IONOSPHERE.
($h_T = h_R = 30$ km, $h = 90$ km, $f = 19.4$ kHz)

CONCLUSION

A comprehensive computational analysis of the vertical component of the electric field strength for individual and multimode propagation of electromagnetic waves at very low frequencies (19.4 KHz and 27 KHz) as a function of distance for different ionospheric conditions and transmitting and receiving antenna elevation configurations has been completed. The analysis proves that the field strength value for the individual modes is dependent on the attenuation constant and the modified height gain factor which have been proved to be dependent on the transmitting and receiving antenna elevation configurations. Consequently, at moderately large distances, fields of higher order modes beomce as significant as that of the first order mode.

The multimode field strength curve displays strong interference phenomenon. The intensity of this interference at a certain distance is dependent upon the transmitting frequency, ionospheric condition and the transmitting and receiving antenna height configurations. When the model interference is strong, the interference pattern displays the occurrence of deep nulls which sometimes occur at distances 800 Km and 2400 Km especially at nighttime when both the antennas are ground-based and the frequency of transmission is 27 KHz.

REFERENCES

1. C. B. Brookes, Jr., J. H. McCable, and F. J. Rhoads, Theoretical VLF Multimode Propagation Predictions NRL Report 6663, December, 1967

2. Peter R. Bannister, VLF/LF/MF Whispering Gallery Propagation Studies, NUSC Technical Report 6503, September, 1981

3. E. Wykes, Test Plan - Strategic Balloon-Borne Communication Experiment, NAVAIRDEVCEN Work Unit Number CY 930, February, 1983

4. James R. Wait, Electromagnetic Waves in Stratified Media, Pergamon Press, Oxford, 1970

5. James R. Wait, Concise Theory of Radio Transmission in the Earth-Ionosphere Waveguide, Reviews of Geophys and Space Phys, 16 No. 3, 320-326, 1978

6. A. D. Watt, VLF Radio Engineering, Pergamon Press, Oxford, 196/

7. Janis Galegs, Terrestrical Propagation of Long Electromagnetic Waves, Pergamon Press, Oxford, 1972

8. M. Abramowitz and I. A. Stegum, Handbook of Mathematical Functions, National Bureau of Standards, Washington, DC, 1964

9. Ya L. Al'Pest and D. S. Fligel, Propagation of ELF and VLF Waves Near The Earth, Consultants Bureau, New York, 1970

APPENDIX A. PROGRAM FOR THE SINGLE MODE FIELD STRENGTH COMPUTATION

```
200 INIT
210 C=54.3
220 R=6.4
230 A=3.5*10↑-3
250 PAGE
260 PRINT "ENTER RECEIVER ALTITUDE IN KM.  ";
270 INPUT H
280 PRINT
290 PRINT "ENTER HEIGHT GAIN FACTOR  ";
300 INPUT C
310 PAGE
320 PRINT "RECEIVER ALTITUDE = ";H;" KM.";
330 PRINT "    HGF = ";C;" DB."
340 PRINT
350 PRINT "RANGE","FIELD STRENGTH"
360 PRINT " KM. "," DB//UV.//KW  "
370 FOR D=200 TO 3000 STEP 200
380 E=C-10*LGT(R*SIN(1.0E-3*D/R))-A*D+C
390 PRINT D,INT(100*E)/100
400 NEXT D
410 PRINT
420 PRINT
430 PRINT
440 PRINT "DO YOU WISH TO CHANGE CONDITIONS AND REPEAT ? (YES,NO)"
450 INPUT T$
460 IF T$<>"NO" THEN 250
470 PRINT "      GOOD BY"
```

APPENDIX B. PROGRAM FOR MULTIMODE FIELD STRENGTH COMPUTATION

```
100 INIT
110 WINDOW 0,3000,0,80
120 DIM R(120),S(120),O(120),E(120),E1(120),E2(120)
130 PAGE
140 A=6400
150 K=0.001555
160 L=0.00656
170 O=0.01519
180 PRINT "ENTER G, H,AND P"
190 INPUT G,H,P
200 PAGE
210 FOR N=1 TO 120 STEP 1
220 D=N*50
230 R(N)=10↑((54.3-10*LGT(A*SIN(D*1.0E-3/A))-K*D+G)/20)
240 S(N)=10↑((54.3-10*LGT(A*SIN(D*1.0E-3/A))-L*D+H)/20)
250 O(N)=10↑((54.3-10*LGT(A*SIN(D*1.0E-3/A))-O*D+P)/20)
260 X=0.916-0.407*D
270 Y=0.809-0.402*D
280 Z=0.799-0.39*D
290 E1(N)=(R(N)*COS(X)+S(N)*COS(Y)+O(N)*COS(Z))↑2
300 E2(N)=(R(N)*SIN(X)+S(N)*SIN(Y)+O(N)*SIN(Z))↑2
310 E(N)=(E1(N)+E2(N))↑0.5
320 NEXT N
330 HOME
340 PRINT "IJJFIGURE   . FIELD STRENGTH VS DISTANCE"
341 PRINT "IH=70 KM,HT=HR=0 KM, F= 19.4 KHZ"
342 PRINT "IX-AXIS DISTANCE IN MEGAMETERS"
344 PRINT "IY-AXIS FIELD STRENGTH IN DB/uV/METER.KW"
350 HOME
355 GOSUB 700
356 VIEWPORT 10,122,10,88
360 AXIS 250,10,0,0
370 MOVE 0,130
380 FOR D=50 TO 6000 STEP 50
```

```
390 IF R(D/50)=0 THEN 420
400 U=20*LGT(R(D/50))
410 DRAW D,U
420 NEXT D
440 MOVE 0,130
450 D=50
460 IF S(D/50)=0 THEN 520
470 T=20*LGT(S(D/50))
480 DRAW D,T
490 D=D+50
500 IF D=6050 THEN 520
510 GO TO 460
520 MOVE 0,130
540 D=50
550 IF O(D/50)=0 THEN 610
560 V=20*LGT(O(D/50))
570 DRAW D,V
580 D=D+50
590 IF D=6050 THEN 610
600 GO TO 550
610 MOVE 0,130
630 FOR D=50 TO 6000 STEP 50
640 IF E(D/50)=0 THEN 670
650 F=20*LGT(E(D/50))
660 DRAW D,F
670 NEXT D
680 PRINT "GGGG"
690 END
700 PRINT "JJJJ 80"
720 FOR I=60 TO 0 STEP -20
730 PRINT "JJJJ  ";I
740 NEXT I
750 PRINT "  ";
760 FOR I=1 TO 3
770 PRINT "                    ";I;
780 NEXT I
790 RETURN
```